EFFECTS OF CYCLIC PRESSURE VARIATION ON PERMEABILITY

A REPORT SUBMITTED TO THE DEPARTMENT OF

PETROLEUM ENGINEERING

OF STANFORD UNIVERSITY

IN PARTIAL FULFILLMENT OF THE REQUIREMENTS FOR THE

DEGREE OF MASTER OF SCIENCE

By

Chuntang Xu

June 2002

I certify that I have read this report and that in my opinion it is fully adequate, in scope and in quality, as partial fulfillment of the degree of Master of Science in Petroleum Engineering.

_____

Prof. Roland N. Horne
(Principal Advisor)

Abstract

The enhancement of seismic stimulation on oil recovery has been recognized and studied for a long time. Based on numerous theoretical studies, modeling approaches, and laboratory scale and field tests, several theories and mathematical models have been developed. However agreement on the fundamental theory behind this phenomenon has not yet been reached.

Pan (1999) developed a series of models of the flow system. She studied the motions in the fluid and solid phases based on homogenizing the Navier-Stokes equation, and by implementing the model with the finite-element technique and numerical analysis. She also provided modeling predictions based on single-phase flow.

To test the elastic wave vibration effect on the single-phase flow and to verify the theoretical predictions at laboratory-scale, two different sets of apparatus were constructed and the single-phase vibration effect was investigated.

Acknowledgments

I would like to give thanks to my adviser, Professor Roland N. Horne, for his constant support, kindness, encouragement and valuable guidance during the course of this research. I also wish to express my appreciation to my friends, Dr. Guoqing Tang, Dr. Kaiwen Li, and Liping Jia for generously providing good ideas for this study.

The financial support from the members of the SUPRI-D Research Consortium on Innovation in Well Testing and from the Department of Petroleum Engineering are gratefully acknowledged.

Contents

List of Tables

List of Figures

Chapter 1

1. Introduction

1.1. Statement of the Problem

Declining oil recovery is of major concern in the oil industry. Common EOR methods have a number of limitations, such as high cost, or possible harmful ecological consequences. Searching for new methods of stimulation is currently an urgent focus to engineers as well as geophysicists. The use of elastic wave excitation has been suggested as an alternative EOR method.

The positive effect of elastic wave vibration on enhancing oil recovery has long been investigated. In the petroleum industry, observations principally in the last 40 years illustrated that elastic waves induced from earthquake or man-made vibration may alter water and oil production. The effect of elastic waves on the permeability of saturated porous media has been studied in numerous laboratory injections. Considerable artificial vibration field-tests carried out in the former Soviet Union went back even to 1950s. Some of these tests illustrated that the dynamic viscosity of the fluid decreased under stimulation. Both laboratory observation and field application have demonstrated that introducing elastic wave signals into porous media may enhance in-situ flow velocity. Based on bench tests and field observations, numerous theories and mathematical models have been provided, which cover fluid dynamics, thermodynamics, nonlinear elastic wave theory and solid dynamics. However, there is no consensus as to the theoretical explanations for the effect of elastic vibration on fluid flow in porous media.

Well testing is a kind of low frequency excitation. However the transient pressure variation is governed by the diffusion equation, which neglects the inertial effects on the fluids. On the other hand, wave theory provides valuable information to describe the solid motion under seismic sweep in which the underlying mechanism is high frequency signal

propagation. Since the fluid flow in the porous medium under excitation is a complicated process, which involves two-phase coupling or multiphase coupling in many cases, the combined study of diffusion analysis and wave interpretation of the elastic vibration is necessary. This combination may provide additional information that is not attainable solely by either well testing or seismic diagnosis.

Based on the homogenization approach, Pan (1999) developed five mathematical models, which apply to the single-phase flow systems with different ranges of physical properties. By numerical analysis, the modeling predictions describing the responses of flow systems under different resonant stimulation were determined. The objective of this study was to test the acoustic vibration effect on single-phase flow at the laboratory scale. By examining the laboratory results of the resonant stimulation frequency, the modeling prediction of Pan (1999) can be verified with real world experiments.

1.2. Literature Review

Theoretical and experimental study on single-phase and multiphase flow in porous media can be traced back to a century ago. Most of the early works were carried out on the modification of Darcy's law. Forcheimer (1901) studied the transient pressure change in porous media by the diffusion equation, based on adding terms of a high order in the velocity. The idea that permeability depends on the absolute pressure was provided by Klinkenberg (1941). Fatt (1959) suggested that the cause of deviations from the prediction of the diffusion equation for the pressure transient lies not in the choice of Darcy's law as the equation of motion but on the existence of dead-end pores which may invalidate the averaged equation of continuity. Bruce et al. (1953) developed numerical procedures to solve a second-order nonlinear partial differential equation, which is introduced by unsteady-state gas flow in porous media. Oroveanu and Pascal (1959) noted that the time derivative of momentum must be included in the equation of motion. Fatt (1960) added a source/sink term to the Darcy-derived equation for a pressure transient. Slattery (1966) discussed local volume-averaging of the continuity equation and of motion over a porous medium. Foster, McMillen and Odeh (1967) illustrated that the equation of motion of a fluid in a homogeneous porous medium might be averaged over a

stationary control volume with the aid of a simple integral transform. They also proposed that for transient flow, the possible dependence of the viscous traction on the time derivative of the average momentum density vector lead to the telegrapher's equation for the averaged pressure field. Odeh and McMillen (1972) derived a nonlinear differential equation, which can describe the space-behavior of a small propagating pressure pulse approximately in an air-saturated porous medium. Haskett, Narahara and Holditch (1986) studied pressure transients analytically utilizing gas flow in small volumes, and stated that the result is very sensitive to both porosity and permeability. Beresnev and Johnson (1994) summarized the theoretical, laboratory and field studies of elastic wave vibrations, which could be dated back to early 1950s, and concluded that the application of elastic-wave excitation to saturated porous media could affect permeability and increase the extraction of hydrocarbons dispersed in the porous spaces.

The development of elastic wave theory to study the acoustic propagation in fluid-saturated porous medium motivated the research of coupling fluid and solid motions to describe the fluid flow in porous medium. Biot (1956) described the elastic wave propagation in saturated porous medium and provided the well-known Biot equation, which later became regarded as a basis for solving wave-propagation problems in porous media. Deresiewicz and Rice (1962) studied wave scattering in a saturated medium by using Biot's equation. Birch (1966) noted a strong nonlinear dependence of modulus on pressure, and a nonlinear stress-strain relation, due to structural discontinuities in the form of cracks, grain boundaries, etc. Stoll and Bryan (1970) and Norris (1989) characterized the wave attenuation mechanism in a poroelastic medium and demonstrated how these effects might be incorporated into Biot's equation. Hamilton (1986) proposed to describe the static and dynamic nonlinear behavior by expanding the modulus in Hook's law as a power series in strain. Bonnet (1987) reviewed some extensions of Biot's equations and derived the complete basic singular solution in the frequency domain for dynamic poroelasticity problems by analogy with thermoelasticity. Zobnin, Kudryavtsev and Parton (1988) explored the flow in inhomogeneous porous systems through the analysis of model periodic structures and obtained an integral differential equation that describes the motion of a viscous fluid in a rigid porous medium of periodic structure.

Depollier, Allard and Lauriks (1988) pointed out that the homogenization process of Biot's equation only applied for a significantly small viscosity fluid. Zinov'yeva et al. (1989) demonstrated that rock showed a large nonlinear response under relatively small strain. Hassanzadeh (1991) developed the Biot acoustic formula by adopting a finite-difference algorithm based on a homogeneous approach. Zhu and McMechan (1991) studied the poroelastic wave equation based on a homogeneous approach. Norris (1992) discussed the analog between the equation of static poroelasticity and the equation of thermoelasticity including entropy, and derived a method of determining the effective parameters in an inhomogeneous poroelastic medium using known results from the literature on the effective thermal expansion coefficient and the effective heat capacity of a disordered thermoelastic continuum. Johnson and McCall (1994) proposed that as the wave propagates, there is a local increase in the density and modulus during compression and a local decrease in density and modulus during rarefaction. Zimmerman and Stern (1995) obtained a series of solutions for the plane compression wave scattering by a spherical poroelastic inhomogeneity medium, which started from Biot's poroelastic model. Dai, Vafidis and Kanasewich (1995) simulated the seismic wave propagation in a porous medium by using a particle velocity-stress, finite-difference method. The modeling enabled them to obtain the particle velocity fields of the volume-averaged solid and fluid motion, and the volume-averaged solid stress and fluid pressure wavefields. Furthermore, this method enabled them to model the seismic response of a heterogeneous medium without introducing numerical approximations of the space derivatives of the physical parameters. Abousleiman et al. (1996) addressed the phenomena of mechanical creep and deformation in rock formations coupled with the hydraulic effects of fluid flow. Johnson et al. (1996) developed a relationship between the nonlinear elastic parameters of rocks and the stress-induced effects on waves propagating in rocks. Li, Cederbaum and Schulgasser (1996) noted that axial fluid diffusion in vibrating beams could easily provide a very strong damping mechanism. Odeh, Chen and Teufel (1997) investigated the rock stress response to the transient fluid pressure in a well with a stationary vertical fracture within the framework of Biot's poroelasticity.

Laboratory observation of elastic wave propagation provided evidence to verify the theoretical and modeling approaches. Brown (1980) pointed out that in the absence of viscosity, the flow pattern minimizes the inertial effects of the fluid; while in the absence of the inertial forces, the flow pattern minimizes the viscous resistivity to flow. At intermediate frequencies, both inertial and viscous forces are significant and the flow pattern must be a compromise that minimizes neither viscous nor inertial effects. Winkler and Nur (1982) illustrated that shear wave attenuation is more sensitive in fully saturated rock than that of compression waves, and the attenuation of both shear waves and compression waves are significantly different in fully saturated rock and partially saturated rock. Williams et al. (1984) showed that both velocity and attenuation of elastic waves could be correlated with porous medium permeability. Chang, Liu and Johnson (1988) predicted the in-situ rock permeability through low-frequency tube wave stimulation. Winkler, Liu and Johnson (1989) indicated experimentally that in oil-field boreholes, Stoneley-wave observations will generally be made in the low-frequency range of theory and suggested that Stoneley wave velocity and attenuation may be indicative of the formation permeability. Auriault (1992) investigated the macroscopic quasistatic description of a deformable porous medium with a double porosity constituted by pores and structures, based on a homogeneous technique. The work exhibited a coupling between the flow and the pores and structures. Auriault (1994) demonstrated that macroscopic behavior of the double porosity medium shows two characteristic pulsations, one corresponds to the quasistatic viscous fluid flow through the microporous medium, and one is the characteristic pulsation of the dynamic fluid flow in the fractures. Bernabe (1997) evaluated the standard frequency dependence of dynamic permeability during the transition from macroscopic viscous flow at low frequency to inertial flow at high frequency, and observed that in networks with large amount of storage pore space, the fluid compressibility could affect the result drastically.

The application of relatively weak elastic wave vibration first attracted the attention of researchers in the USSR and USA in the late 1950s. The peak of activity dates to the early 1970s in US and the 1970s and 1980s in the USSR. Bredehoeft (1967) illustrated that analysis of the water-level fluctuations caused by the earth tide can be used to compute

the specific storage and the porosity of the aquifer. Brace et al. (1968) suggested a nonsteady state technique, or pressure pulse technique to determine the permeability of tight cores. Freeman and Bush (1983) stated that the pressure pulse permeability determination is stress sensitive at low pressure and the measurement should be made at net reservoir overburden to estimate reservoir permeability accurately. Chen and Stagg (1984) evaluated the pulse-decay measurements by using a semilog analysis technique. Crosnier, Fras and Jouanna (1985) applied harmonic techniques to a physical model simulating fractured media, and proposed a mathematical method to determine the parameters, such as the number of sets of cracks and the different thickness of each set, from the spectral signatures. The comparison between theory and laboratory tests showed a good fit in the medium range of frequencies. Amaefule et al. (1986) outlined experimental protocols for accurate determination of liquid permeability in low quality rocks, and verified that the pulse-decay technique is well suited for determining the effective oil and water permeability in low quality cores. The paper stated that the oil and water permeability for some low quality cores is stress-sensitive. Charlaix et al. (1988a, 1991) did a series of experimental studies on the dynamics of fluid flow in capillaries by using harmonic techniques. The dynamic permeability was measured at a frequency range of 0.1 Hz to 1 Hz. Dean et al. (1991) introduced a method to monitor compaction and compressibility changes in offshore chalk reservoirs by measuring the tidal effect in the reservoir. Sharma (1995) verified experimentally that application of ultrasonic energy is capable of partially removing wellbore damage arising from the invasion of mud particles and significantly increasing the permeability in the near-wellbore zone. Nikolaevskiy et al. (1996) found that a vibration whose frequency is dictated by reservoir lithology, fluid saturation, and layer stratification altered oil and water production characteristics and could enhance oil production near the residual oil saturation and increase water production near the immobile water saturation. Tencate et al. (1996) compared the measurement of linear and nonlinear wave propagation in Berea sandstone with numerical results, suggesting that hysteresis and end-point memory likely play prominent roles in wave propagation in rocks. Pinilla, Trevisan and Tinoco (1997) modeled the oceanic tidal effects on an infinite reservoir by coupling geomechanic principles with

equations for fluid flow in a deformable porous media. Kouznetsov et al. (1998) reported an increased oil recovery and oil/water ratio by using powerful surface-based vibroseismic sources, and pointed out that decreased water cut was caused by the reduction in water/oil interfacial tension and increase in the relative permeability of the oil. Dusseault et al. (2000) showed that when a porous medium undergoing flow at a constant head was excited appropriately, the flow rate would increase. Westermark, Brett and Maloney (2001) summarized laboratory and field tests and pointed out that orbital vibrations were capable of producing both shear and compression wave energy at frequencies and intensities that can be engineered to provide enhanced fluid flow.

The study of the effects on oil mobility produced by low frequency waves is of special interest because of their potential application to the reservoir. The laboratory and field tests on elastic-wave excitation of oil production were reviewed in detail by Beresnev and Johnson (1994). Duhon (1964) reported a laboratory study regarding the influence of ultrasonic energy on liquid flow through porous media. An increase in oil recovery was observed under ultrasonic excitation, and the permeability of $\boldsymbol{k}_{water}/\boldsymbol{k}_{oil}$ in the absence of sound was found to be greatly reduced after sound was applied. Cherskiy et al. (1977) measured the permeability of rock saturated with fresh water in the presence of an acoustic field. The permeability of the sample increased sharply within a few seconds after the beginning of the pulse-mode treatment. A few minutes after removal of the sound field, the permeability decreased to the value before excitation. Dyblenko et al. (1989) observed the enhancement of kerosene displacement by water in a reservoir core sample by applying sound at a frequency of 200 Hz. The mobility of residual oil increased and the permeability to water decreased during the excitation. Snarskiy (1982) reported a 19 percent increment of oil displacement for fine–grained quartz sand exposed to 9 - 40 Hz sound field, and observed the effect was frequency dependent. Sherborne (1954), Medlin et al. (1983), Simkin (1985) and Kuznetsov et al. (1986) showed that vibration treatment may be effective in combination with gas or fluid injection in a producing formation.

Chapter 2

2. Problem Description

The character of single-phase flow under steady injection honors Darcy's law. In steady flow, all of the related parameters, such as the permeability of the flow system, in-situ flow velocity and porosity are all static. When a perturbation signal is introduced in the flow system, even thought the averaged injection rate is constant, the pressure drop in the porous media may deviate from the differential pressure at steady state. It has been suggested in some theories (Beresnev, et al., 1994) that the reduction in surface tension caused by the differential velocity between the rock matrix and the pore fluid is the fundamental source of the increased permeability. Other researchers (Mingyuan, et al. 1999) attributed the permeability variation to the wettability reversal of the rock system under elastic excitation. Elastic wave theory holds that, under elastic vibration, two kinds of waves can be induced in the flow system. One is the shear wave, which propagates dominantly in the rock matrix. The other is the compression wave, which is transmitted prominently in the pore fluid. The shear waves and compressional waves travel at different velocity. When both waves are present, there will be times during the propagation that the two waves will reinforce each other vectorially. The coupling action may result in greater permeability increases than either wave could produce alone.

It has also been suggested (Nikolaevskiy, 1997) that the surface films absorbed on the pore boundaries may be destroyed under mechanical stimulation. Thereby, the effective cross-section of pores would increase. In addition, the propagation of shear waves in the solid matrix can induce the oscillation of the solid particles along the interface of the pore structures, and the mobilization of in-situ clay fines. Both of the actions would be helpful to improve the effective conductivity of the flow system and enhance the local porosity, which in macroscopic terms would be manifest as an enhancement of the rock permeability.

There is no doubt about effect of elastic wave effect on oil recovery. Considerable theoretical and experimental work has been done to describe this phenomenon. However, currently there is no consensus on the theoretical explanation of the effect.

2.1. Modeling Development

Pan (1999) investigated single-phase intermediate frequency stimulation by modeling the coupling of the solid and liquid motions at pore scale. Starting from the basic Navier-Stokes equation, which is suitable for describing fluid flow in the pores, and combining with the homogenization process, Pan (1999) derived five separate characteristic macroscopic models. In the derivation of the macroscopic quasistatic behavior, the saturating fluid is assumed viscous and Newtonian. The five models are:

- Model *I*: Acoustics of Empty Channels
- Model *II*: Acoustics of a Fluid in a Rigid Channel
- Model *III*: Diphasic Macroscopic Behavior
- Model *IV*: Monophasic Elastic Behavior
- Model *V:* Monophasic Viscoelastic Behavior

2.2. Modeling Prediction

The theoretical and numerical results of Pan (1999) showed that the response of a porous medium to harmonic perturbations depended on the parameters of the pore structure, the properties of the fluid and the frequencies of the excitation signal. The elastic wave vibration had positive impact on fluid flow under harmonic perturbation. Pan (1999) studied the natural frequency of a dry porous medium theoretically, and verified numerically that at certain resonant frequencies, the perturbation demonstrated positive effects on the in-situ flow velocity. Table 2.1 illustrates the numerical prediction of the natural frequencies of the rocks by Pan (1999). The parameters in the table are dimensionless. In the derivation, the natural frequency was assumed to be determined solely by the porous medium porosity.

Table 2.1: Natural frequencies of porous media as a function of porosity (Pan, 1999).

ϕ_c	ω_{01}	ω_{11}	ω_{02}	ω_{12}	ω_{21}	ω_{03}	ω_{22}	ω_{13}	ω_{23}
0.20	0.680	1.712	2.041	2.575	3.214	3.401	3.746	3.746	4.630
0.25	0.907	1.814	2.721	3.142	3.270	4.534	4.156	4.799	5.516
0.33	1.360	2.708	4.081	4.373	3.423	6.802	5.150	6.981	7.492
0.50	2.721	3.142	8.162	8.312	4.156	16.603	8.746	13.694	13.962

Pan (1999) analyzed the effective parameters obtained by volume-averaging. She also studied the sensitivity of the macroscopic behavior to both the porous medium properties and to the frequencies of the perturbation signal. The natural frequency prediction is directly relevant to this study, and will be valuable to evaluate a potential EOR method by harmonic stimulation.

2.3. Objective of Experimental Investigation

Based on the theoretical prediction, this study looked mainly at the elastic vibration effect on the fluctuation of the rock permeability, under single-phase injection at laboratory-scale, and sought to provide a reasonable explanation for this phenomenon, and also to provide physical verification of the numerical prediction by Pan (1999).

Another objective of this study was to look at alternatives to traditional well-testing interpretation methods. Well test is a kind of low or intermediate frequency excitation of the reservoir. Consequently, an accurate prediction of the interrelation between the dynamic permeability and the excitation frequency could enhance the range of variables determined from well test interpretation.

Principal study procedure:

1. Design a reliable laboratory-scale mechanical excitation apparatus for single-phase flow. Also achieve the capacity to expand to multiphase and more complicated excitation tests.

2. Perform low-frequency elastic vibration injection at frequencies from 0.1 Hz to 10 Hz, monitor differential pressure variation under different frequency vibration.

3. Vibrate a loose sand pack to test the effect of oscillation in solid-phase on single-phase flow. Comparing the elastic vibration effect on core samples with significantly different physical properties.

4. Monitor the elastic vibration treatment effect on upstream and downstream pressure and phase shift, and interpret the relationship of the phase shift and vibration frequency.

5. Predict the elastic wave propagation in the solid phase by interpreting the differential pressure variation and upstream and downstream pressure phase response.

6. Measure in-situ pressure and local flow velocity variation.

7. Interpret the resonant frequency theory for porous media with different physical properties at laboratory scale.

8. Provide reasonable physical explanation for the elastic wave effect on single-phase flow, and predict the response on reservoir scale.

Chapter 3

3. Experimental Apparatus and Procedure

This section discusses the procedure for achieving sine-wave shape pressure pulse excitation in the laboratory. Two kinds of apparatus with different functions were developed: (1) pressure pulse by solenoid valve, and (2) pressure pulse by electromagnetic exciter.

3.1. Pressure Pulse by Solenoid Valve (PPSV)

For PPSV, the solenoid valve was placed at either the inlet or outlet end of the flow system. The pressure variation in the system was controlled by opening and closing the valve. The theoretical operation frequency of the valve is 0.2 – 2 Hz, therefore, it is suitable to low intermediate frequency stimulation. This configuration is shown in Figure 3.1.

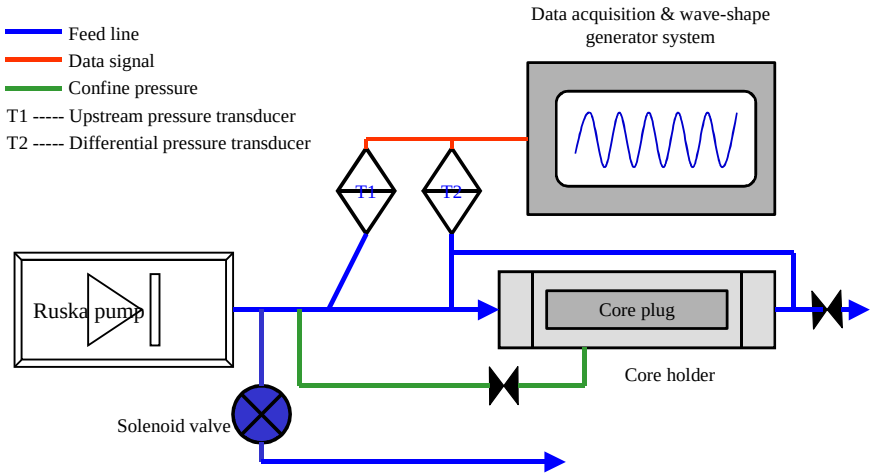

Figure 3.1: Flow chart of excitation by solenoid valve.

This design is simple, easy to operate, and applicable to many kind of fluids. A defect is the difficult in determining the flow rate. The valve operation is achieved by closing and opening an electromagnetic valve cone; therefore a delay between the electronic signal

and the electromagnet operation is inevitable. For instance, if the designed vibrating frequency is 1 Hz, the theoretical duration of opening or closing the valve is 1 second. However, the actual open time is 0.95 seconds. The 0.05 seconds is consumed in opening and closing the valve. Within the 0.05-second interval, the flow velocity gradient approaches to infinity from zero; the flow characteristic is definitely different from the flow at the stabilized stage. Furthermore, under high frequency operation, the valve failed to work properly, which resulted in an unstable flow rate. Consequently, this design was substituted by a new arrangement.

3.2. Pressure Pulse by Electromagnetic Exciter (PPEE)

The stimulation source in the PPEE is generated by the combination of an electromagnetic exciter (Figure 3.2), driven by an electronic signal amplified through a power amplifier, and a hydraulic cylinder (Figure 3.3). The theoretically applicable frequency of the exciter ranges from 0.1 to 10 kHz. The flow chart of the design is illustrated in Figure 3.4, and the experimental apparatus is shown in Figure 3.5. Three kinds of wave signals, such as sinusoid, triangle and square wave can be applied to the exciter. A function generator is used to generate wave signals. After being amplified by a power amplifier, the wave signal is fed to the exciter. Driven by the exciter, the dual action hydraulic cylinder transforms the kinetic energy into hydraulic power thus generates cyclic pressure pulses in the flow system.

Figure 3.2: Electromagnetic exciter.

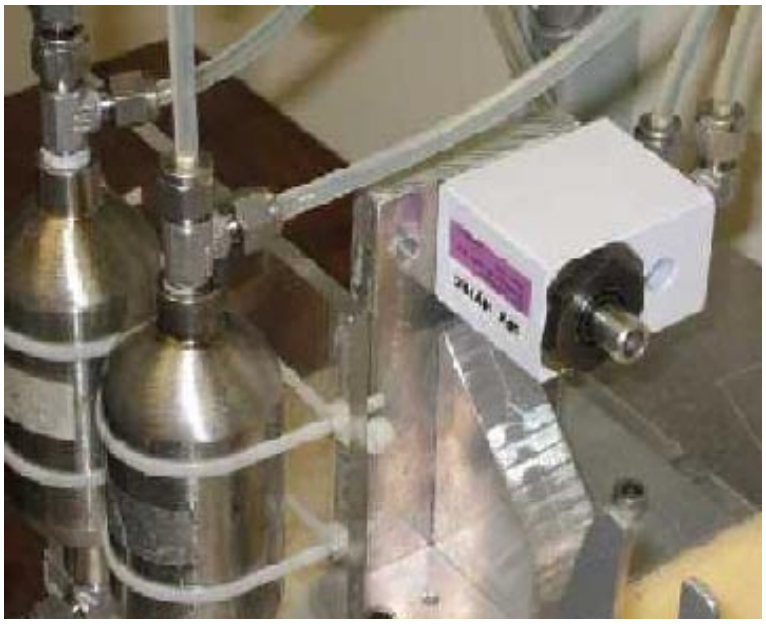

Figure 3.3: Dual action hydraulic cylinder.

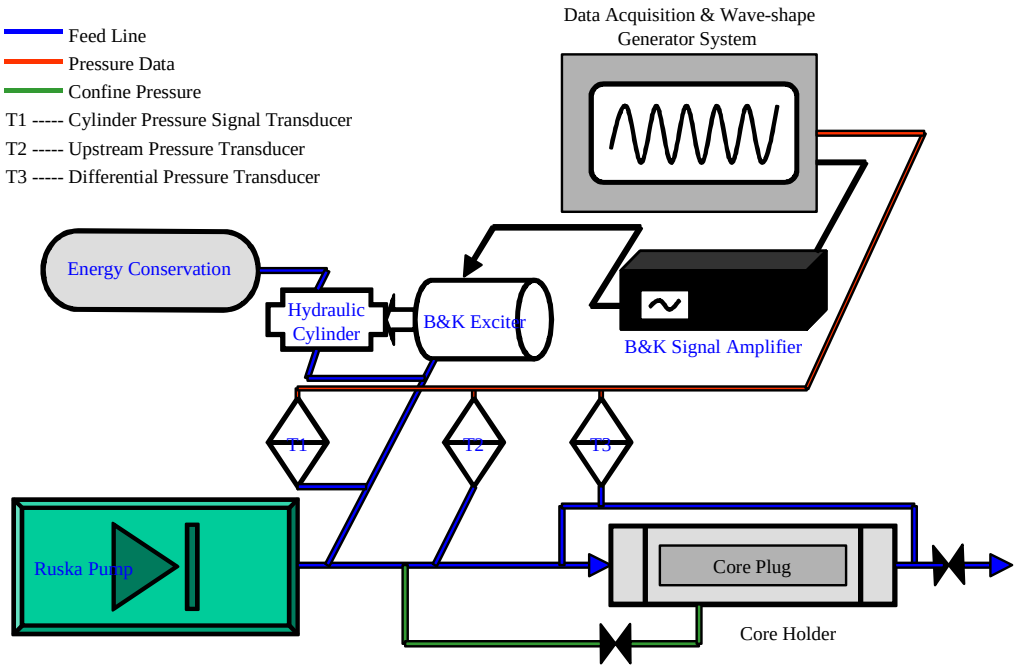

Figure 3.4: Flow chart of excitation by electromagnetic exciter.

Figure 3.5: Overview of apparatus.

3.3. Rock Physical Properties and Stimulation Parameters

The rock samples used were a Berea sandstone plug and a ceramic core. The physical parameters of the core samples are listed in Table 3.1:

Table 3.1: Physical properties of the rock samples.

Rock	d (cm)	l (cm)	v_T (ml)	v_p (ml)	ϕ (%)	k (md)	q (ml/min)
Berea sand	*2.54*	*9.00*	*45.6*	*9.58*	*21.0*	*450*	*19.8*
Ceramic	*2.54*	*7.77*	*39.4*	*9.84*	*25.0*	*2*	*0.2*

Experiment Parameters:

Flow media: degassed and distilled water

Injecting pressure: *30 -- 50 psi*

Frequency range: *0.2 – 5.0 Hz*

Pressure variation amplitude: *~5psi*

Confining pressure: *100psi*

3.4. Experimental Preparation

One important point that needs to be emphasized is with regard to the effect of excitation on the mobilization of clay fines. Under steady injection, the clay fines are immobile. During an excitation test, the clay fines will be mobilized. Therefore, the permeability variation will be partially attributable to the mobilization of the clays. To study the pure influence of the rock matrix vibration, the rock needs to be fired to eliminate the clay mobilization. In this project, the rock permeability fluctuation was ascribed to the joint effect from clay fine mobilization and pore structure change; therefore the rock sample was not fired.

3.4.1. Porosity Measurement

After the rock sample was dried at $105^{o}C$ over 8 hours and the weight was constant, it was saturated with degassed distilled water for another 8 hours. The weight difference between the wet core and dry core was used to infer the porosity of the sample. The precision of porosity evaluation by this method is acceptable.

3.4.2. Permeability Measurement

The water saturated rock sample was wrapped with a rubber sleeve and then installed in the core holder for test. To avoid the influence of air on the water flow, and salt inhibition on shale dilation, degassed distilled water was used as the flowing fluid to keep single-phase flow.

The system was flooded at a constant flow rate. Flow rate and pressure drops were measured. Combining the known rock geometric parameters, water viscosity and using Darcy's law, the rock permeability can be calculated. To have an accurate measurement of the rock permeability, gas-flooding calibration was conducted in advance.

3.4.3. Elastic Vibration

After obtaining porosity and permeability, the excitation test was initiated. The following steps were taken:

1. Adjusting the injection pressure to 50psi or below;
2. Turning on the function generator and tuning to the expected frequency;
3. Turn on the power amplifier and slowly increasing the input current;

During this process, the pressure variation at the inlet of the core was monitored using Labview and the pressure variation amplitude was controlled to be less than 10% of the steady injection pressure. Another point to be mentioned is the need to keep the output current to the exciter less than the current limit value of the power amplifier. When the CURRENT lights red on the LED indicator, the instrument stops working.

There are two ways to generate the wave signal: one is to use the wave function provided by Labview package. The wave signal created by this way is smooth and accurate, and is easy to operate. The drawback is that the signal generator and the data acquisition device share the same bus. For high-frequency stimulation or large rate of data recording, there would be conflict between the output wave signal and data reading and recording. The second way is to use the external function generator to generate the wave signal; this way is reliable, but the signal accuracy is relatively low. Both methods can be used for sinusoid, square, and triangle wave.

The pressure was monitored and recorded to a text file or Excel file by the Labview software, (Figure 3.6).

One important point for the experiment needs to be noted. When measuring the pressure response under different stimulation frequencies, the time interval between two adjacent measurements must be long enough for the flow system to return to a stable condition. Under stimulation, even though the excitation amplitude is small (only 10% of the injecting pressure), the induced oscillation in the rock matrix may still exist and may take some time to recover. Based on current tests, it was found that it took about five to six minutes for the system to go back to a steady state (for the ceramic core). The time interval is not constant, and it is a function of stimulation intensity and the rock

dimensions. The higher the stimulation intensity or the larger the rock size, the longer time interval is required for the recovery.

To accurately evaluate the deviation of inlet and outlet pressure from a steady state, the steady-state pressure at different stimulation conditions needs to be measured separately. This is because after excitation, the flow condition could be changed

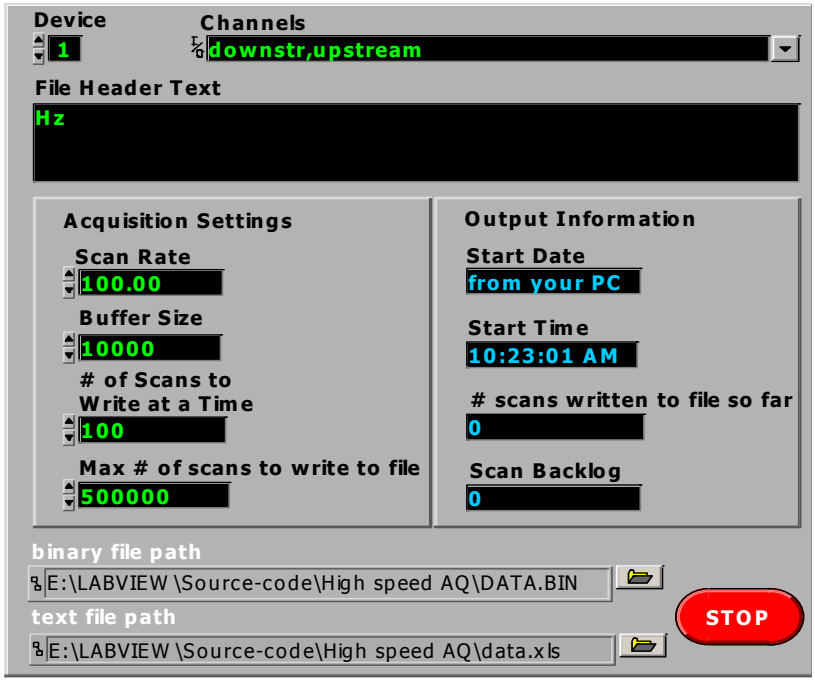

Figure 3.6: Labview data acquisition window.

Chapter 4

4. Results and Discussion

This chapter examines the experimental results regarding the effect of excitation frequency on the permeability variation at single-phase flow. Restrained by the output power of the exciter, the injecting pressure was controlled below 50psi, and the excitation magnitude was limited to 5~10 psi. Test frequency covered a range 0.2 Hz to 5.0 Hz.

4.1. Data Interpretation Technique

The measured data are scattered and not easy to analyze quantitatively. A moving-window average technique was adopted in the data interpretation, by estimating one data point value by using the averaged value of three or five adjacent data points.

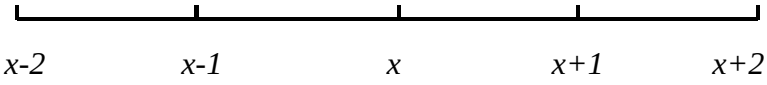

Figure 4.1: Data smoothing technique.

As illustrated in Figure 4.1, we interpret the data point *x*, instead of using the value of *x* directly, by denoting $x = sum(x_i)/n,\ i=1\sim n,\ n=3\ or\ 5$. This technique is useful to interpret the trend of the data points, or identify important characteristics of the data sequence.

In this project, the data smoothing technique was applied only to clarify the phase delay phenomenon. For pressure magnitude interpretation, using the smooth technique might conceal some important information, so the original measured data was considered instead of the smoothed data. For example, under harmonic perturbation, theoretically the in-situ flow velocity may change sharply (Pan 1999, Chapter 5: Analysis of Results). In macroscopic terms, this effect would be visible as the differential pressure oscillation. However the data smoothing technique could smooth out this significant detail.

The interpretation of the upstream, downstream and differential pressure, upstream and downstream pressure phase and dynamic permeability will be addressed in the following sections.

4.2. Pressure Signal Interpretation

Upstream pressure and downstream pressure denote the pressure at the inlet end and outlet ends of the core plug. Differential pressure refers to the pressure drop from one end of the core plug to the other. Under steady single-phase flow, the upstream, downstream and differential pressures are constant. Therefore, any changes in the magnitudes of these three pressures under vibration can be treated as the effect of the excitation. Generally, these three pressures can be measured directly by pressure transducers. However in this study, since they are affected by the phase change of the pressure signal at the two ends of the core sample, the direct observations of the differential pressure signal are scattered and difficult to analyze. Therefore the differential pressure is interpreted from the difference between the measured upstream and downstream pressures instead.

At steady state, the inner friction between the solid phase and the liquid phase along the interfaces of the tortuous channels and pore structures balances the injecting pressure; the kinetic energy will be transferred into thermal energy. In macroscopic terms, this phenomenon results in a pressure drop along the core sample. For homogeneous and isotropic rock samples, the pressure drop is distributed linearly along the porous medium. Darcy's law is sufficient to describe this process.

Under excitation, the cycling variation of injecting pressure may induce solid phase oscillation, change of pore geometric shape, and mobilization of clay fines in the rock matrix. The mobilization of solid particles along the channels or well-connected pore structures can affect the smoothness of the channel interface significantly, which in turn results in the variation of inner friction. Consequently, the common definition of the fluid dynamic viscosity, which is assumed as a constant, is not applicable. A new substitute, which couples the fluid and solid motion to describe the dynamic viscosity, should be applied. Because the oscillation in the solid phase is determined by the perturbation

frequency, solid phase properties, and the pore geometric structure, the microscopic characteristics of the solid matrix should be included when we study the flow property.

When the stimulation frequency matches the natural frequency of the solid matrix, the vibration is referred to as harmonic perturbation. At the microscopic scale, the harmonic shear wave in the porous media results in the geometric shape change of the pore structure or the channels in the solid phase. Meanwhile, in the fluid phase, the propagation of the harmonic compression wave causes harmonic pressure fluctuation inside the channel and pore space. There will be times when the two harmonic waves will reinforce each other, and the combined action may result in greater permeability increases than either wave can produce alone. At the macroscopic scale, the coupling action of solid and liquid phase is observed as a fluctuating flow rate under constant differential pressure, or fluctuating pressure drop along the core sample at constant injection rate.

Generally, the local properties of the porous medium, such as porosity and permeability, will be dynamic under vibration. Therefore, the traditional Darcy's law should be modified to interpret the flow properties under these conditions.

In this study, the stimulation injection was run following the steady-state flow. To be consistent in comparison, the two flows had identical injection condition, such as flow rate etc. The recorded upstream and downstream pressure is hard to interpret, therefore, the averaged pressure was compared with the pressure at steady state.

4.2.1 Upstream Pressure Response under Vibration

Figures 4.2 - 4.3 show the comparison of the upstream pressure under vibration with steady state injection for the ceramic core. Under most of the tested frequencies, the measured pressure signal is distributed evenly above and below the pressure curve under steady state, which indicates that the excitation has no apparent effect on the flow. Checking the averaged pressure, the averaged value is almost the same as at steady state. Slight deviations of the averaged pressure from the steady state occur at 0.5 Hz, 1.5 Hz and 3.0 Hz. The magnitudes of the decreases are from 0.1 to 0.3 psi.

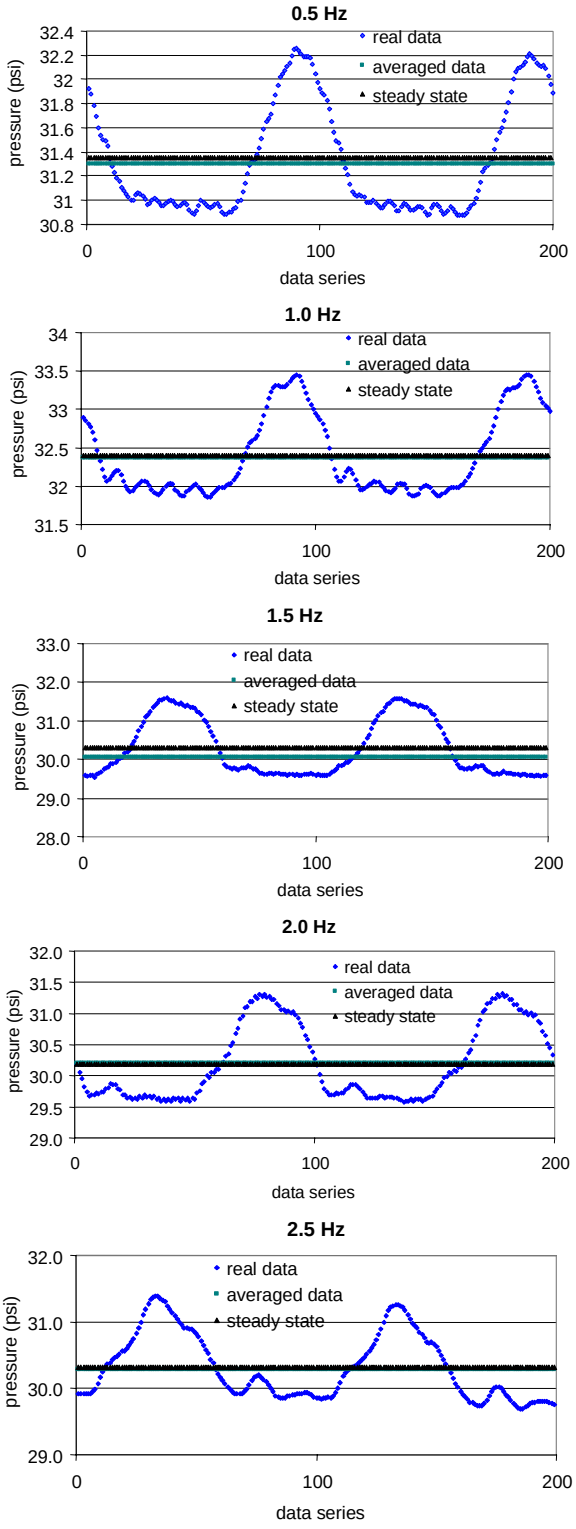

Figure 4.2: Upstream pressure under excitation (0.5 - 2.5 Hz, ceramic core).

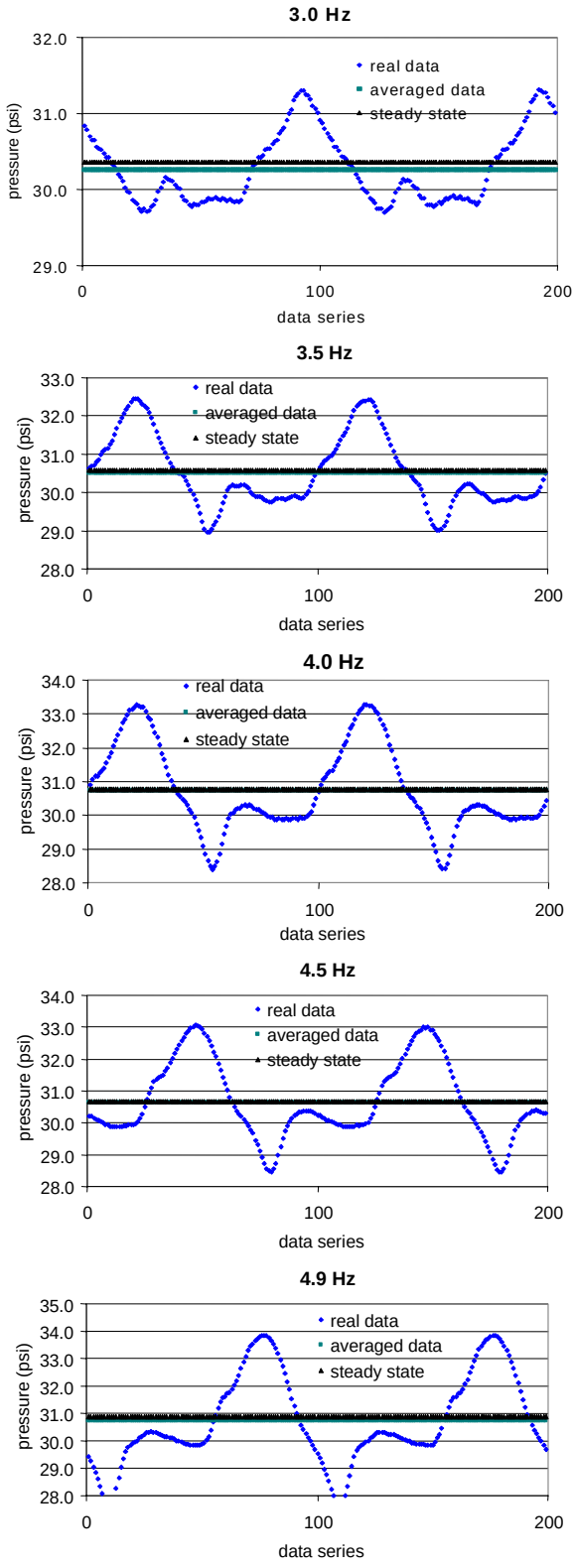

Figure 4.3: Upstream pressure under excitation (3.0 - 4.9 Hz, ceramic core).

The difference of the averaged upstream pressure under stimulation and at steady injection for the ceramic core plug is illustrated in Figure 4.4. The vibrated upstream pressures at 1.7 Hz - 2.0 Hz and at 4.9 Hz increased compared to that at steady state. Consistent with the observation in Figures 4.2 – 4.3 the maximum reduction of the averaged pressure is at 0.5 Hz, 1.5 Hz and 3.0 Hz respectively. The decrease of the upstream pressure indicates a reduced flow resistivity of the ceramic core, while the increased upstream pressure illustrates a negative effect of the vibration on the flow.

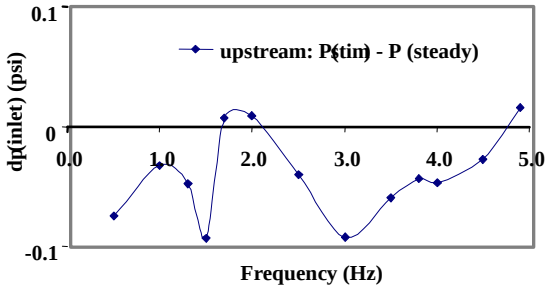

Figure 4.4: Upstream pressure vs. excitation frequency (ceramic core).

The upstream pressure responses for the Berea sandstone, at steady state and under vibration, are demonstrated in Figures 4.5 – 4.6. Similar to the ceramic core plug, the measured upstream pressures are distributed evenly above and below the pressure at steady state. The average pressure keeps the same value as at steady injection for most of the tested frequencies. Slight deviations occurred at 2.0 Hz, 2.5 Hz and 3.0 Hz, at which the average pressure increased slightly. The increased average upstream pressure indicates that the flow resistance in the porous medium was boosted under vibration.

Figure 4.7 illustrates the difference of the upstream pressure under vibration and at steady state for the Berea sandstone. The difference is greater than zero (or the averaged pressure is higher than at steady state) under most of the studied frequencies, which indicates that the flow impedance increased in the porous medium at these frequencies. The maximum impedance occurred at 2.5 Hz. At this frequency, the vibration produced a strong negative effect on the flow.

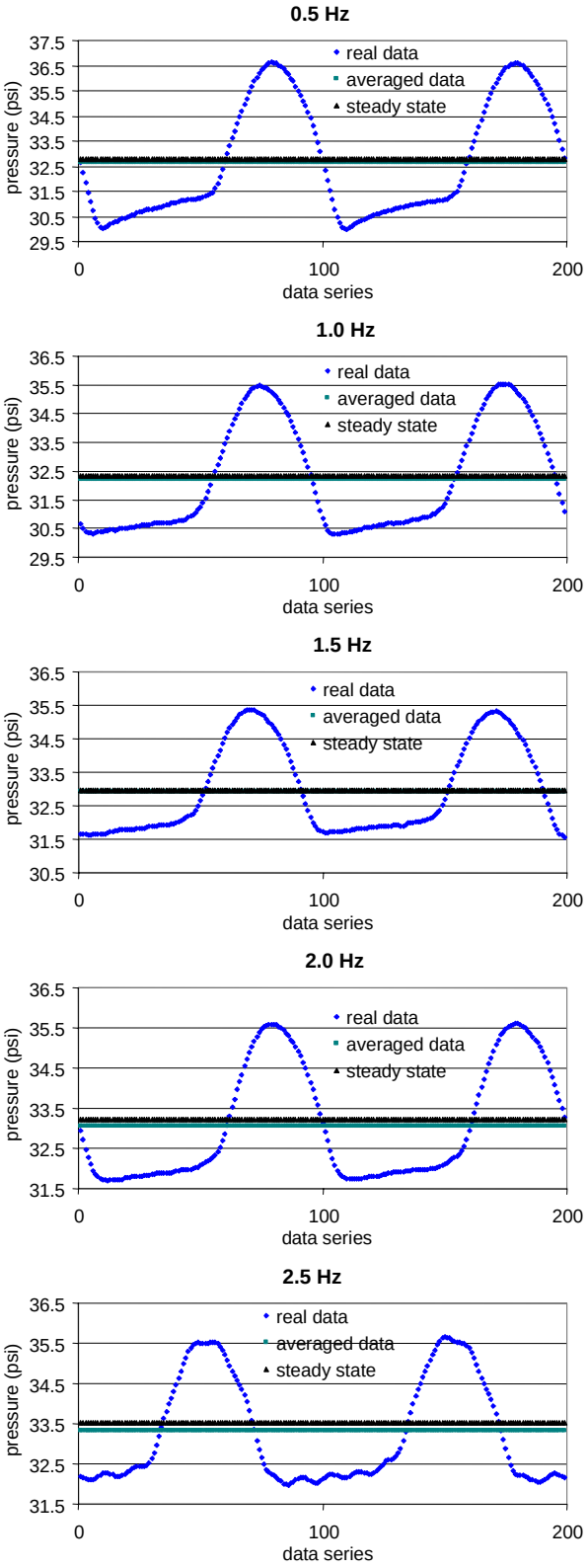

Figure 4.5: Upstream pressure under excitation (0.5 – 2.5 Hz, Berea sandstone).

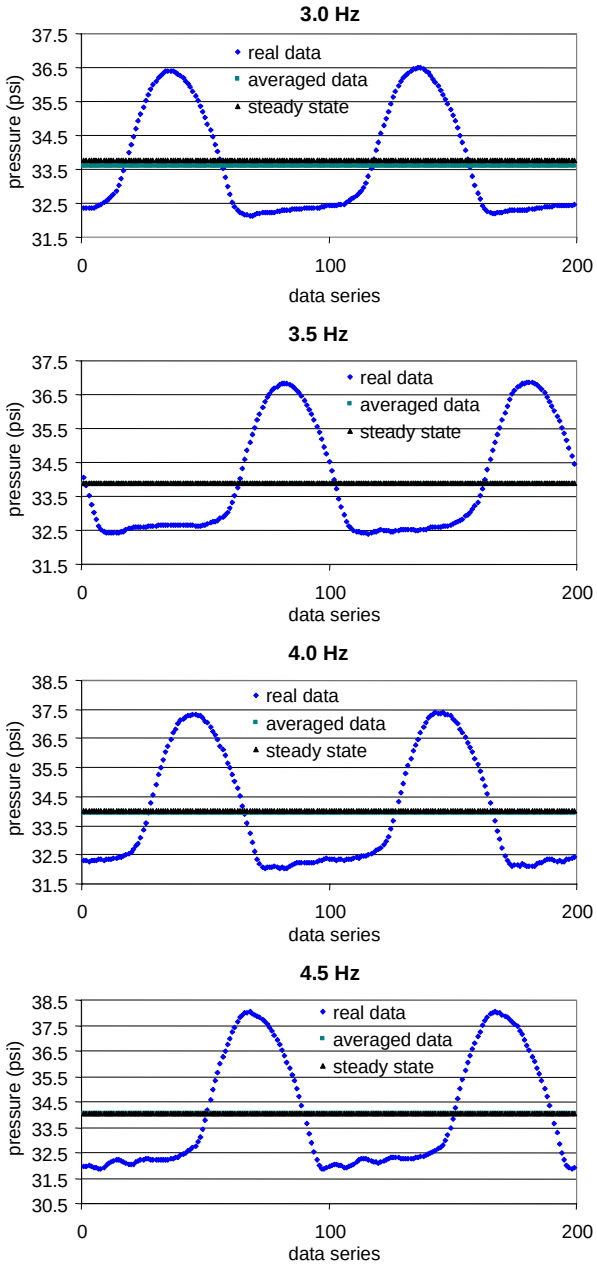

Figure 4.6: Upstream pressure under excitation (3.0 - 4.5 Hz, Berea sandstone).

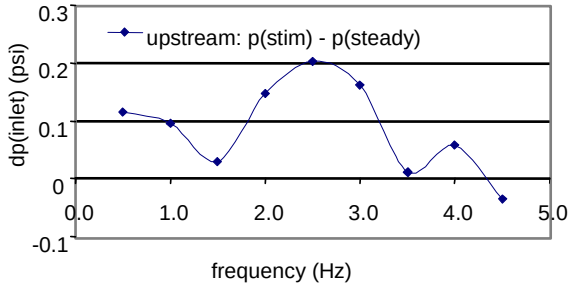

Figure 4.7: Upstream pressure vs. excitation frequency (Berea sandstone).

Based on observation of the upstream pressure response, the vibration exhibits negative effect for frequencies in the range of 1.7 Hz to 2.0 Hz and above 4.5 Hz, and positive stimulation effect under the rest tested frequencies. The excitation of the Berea sandstone shows negative effect for frequencies under 4.0 Hz, and positive effect for frequencies above 4.0 Hz.

4.2.2 Downstream Pressure Change under Stimulation

For the ceramic core plug, the responses of the downstream pressure, compared to that during steady injection are shown in Figures 4.8 – 4.10. Unlike the response of upstream pressure, most of the measured data is above the steady-state downstream pressure. Comparing the average outlet pressure with that at steady injection, there is about 0.05 to 0.2 psi increment for the vibration cases.

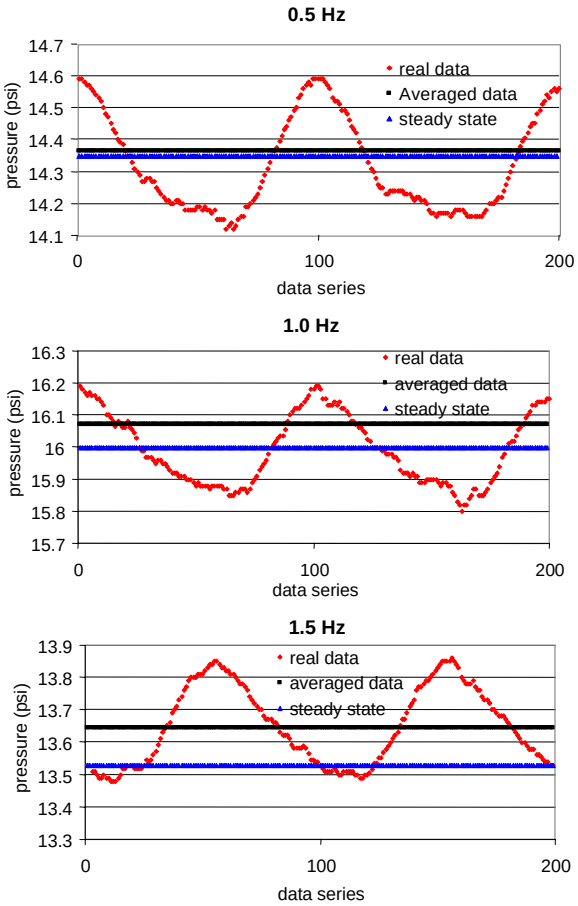

Figure 4.8: Downstream pressure under excitation (0.5 – 1.5 Hz, ceramic core).

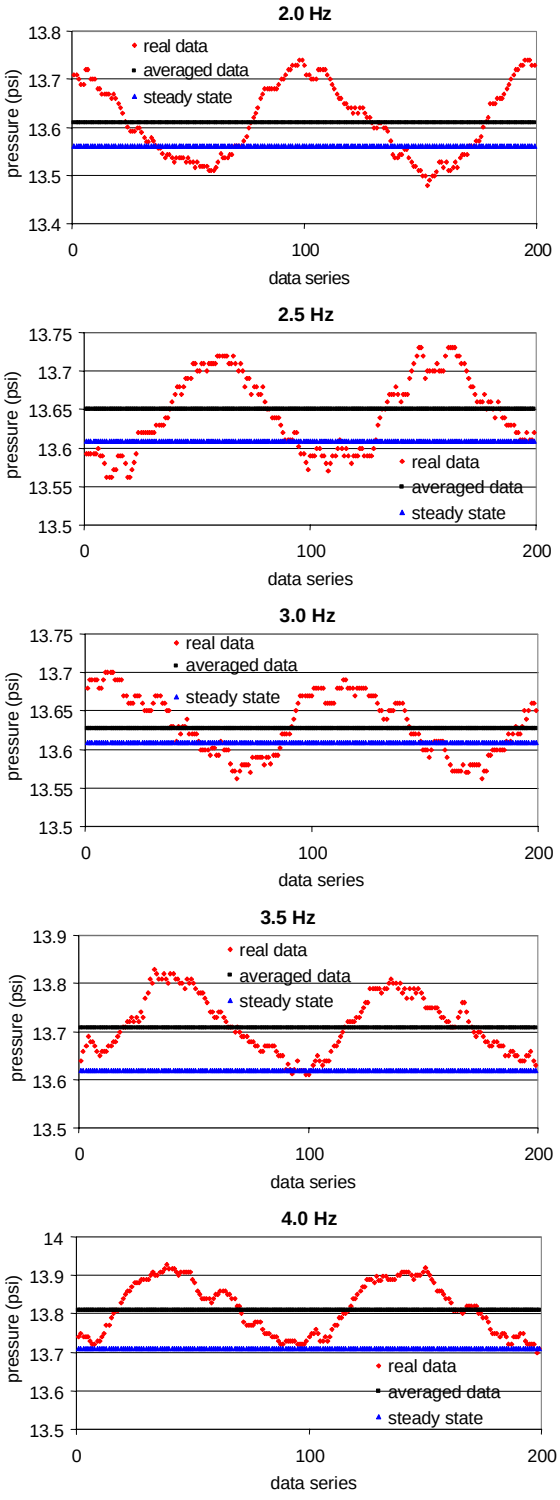

Figure 4.9: Downstream pressure under excitation (2.0 – 4.0 Hz, ceramic core).

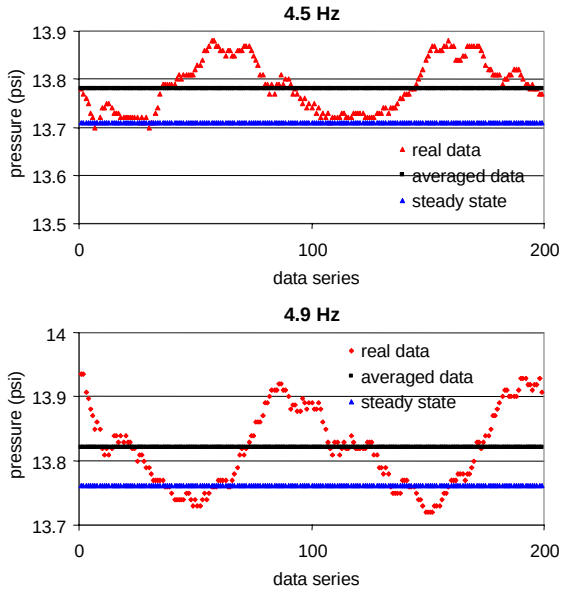

Figure 4.10: Downstream pressure under excitation (4.5 – 4.9 Hz, ceramic core).

Figure 4.11 shows the difference between the downstream pressure under vibration and that at steady state for the ceramic core. As in Figure 4.8 – 4.10, the averaged downstream pressure is greater than at steady state under the investigated frequencies. This illustrates that the pressure drop in the porous medium decreased under vibration, and the excitation reduced the flow resistance of the medium.

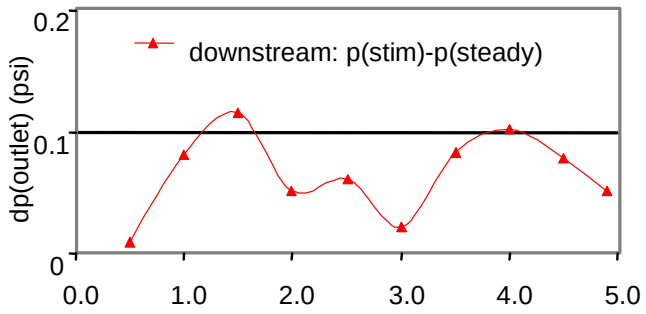

Figure 4.11: Downstream pressure vs. excitation frequency (ceramic core).

The downstream pressure responses for the Berea sandstone are quite different from those in the ceramic core. In Figures 4.12 – 4.13, the average pressure shows some variations. At 0.5 Hz and 1.5 Hz, the average pressure is the same as at steady state, which would indicate that the vibration has no effect on the flow. At 1.0 Hz, 2.0 Hz and 2.5 Hz, the average value is lower than at steady state, an apparent indication of increased flow

resistance in the porous medium. From 3.0 Hz to 4.5 Hz, the averaged downstream pressure is higher than at steady state, which implies reduced flow impedance.

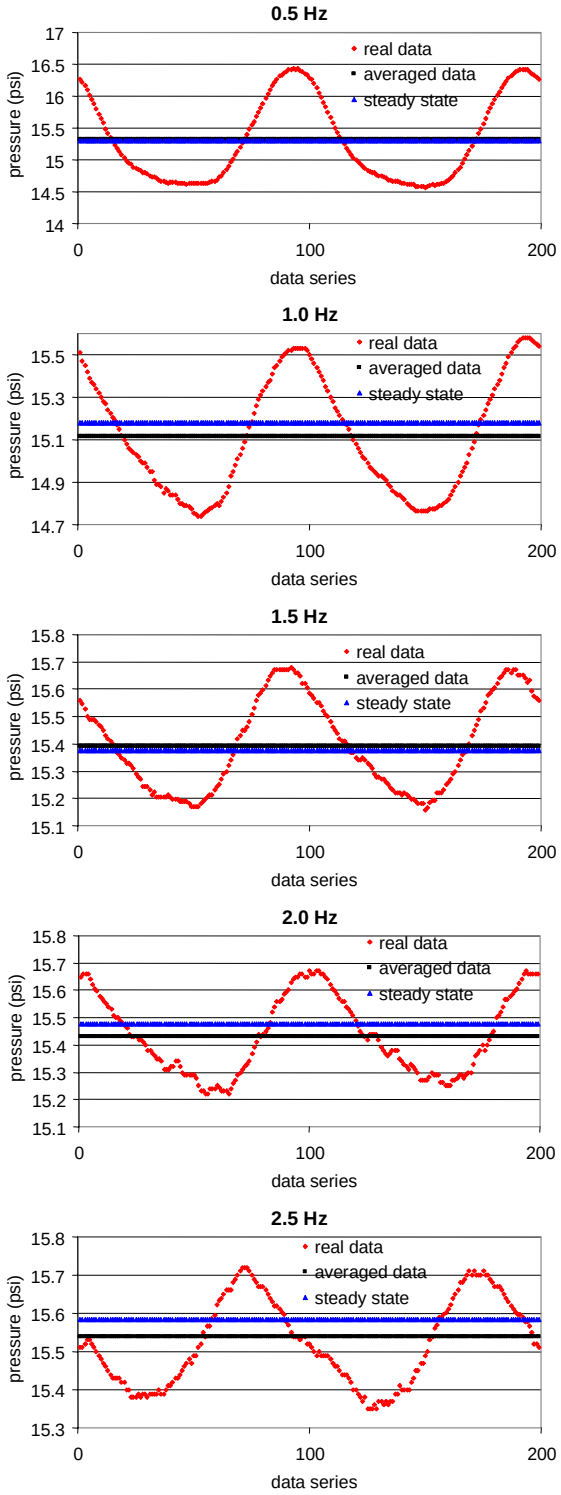

Figure 4.12: Downstream pressure under excitation (0.5 - 2.5 Hz, Berea sandstone).

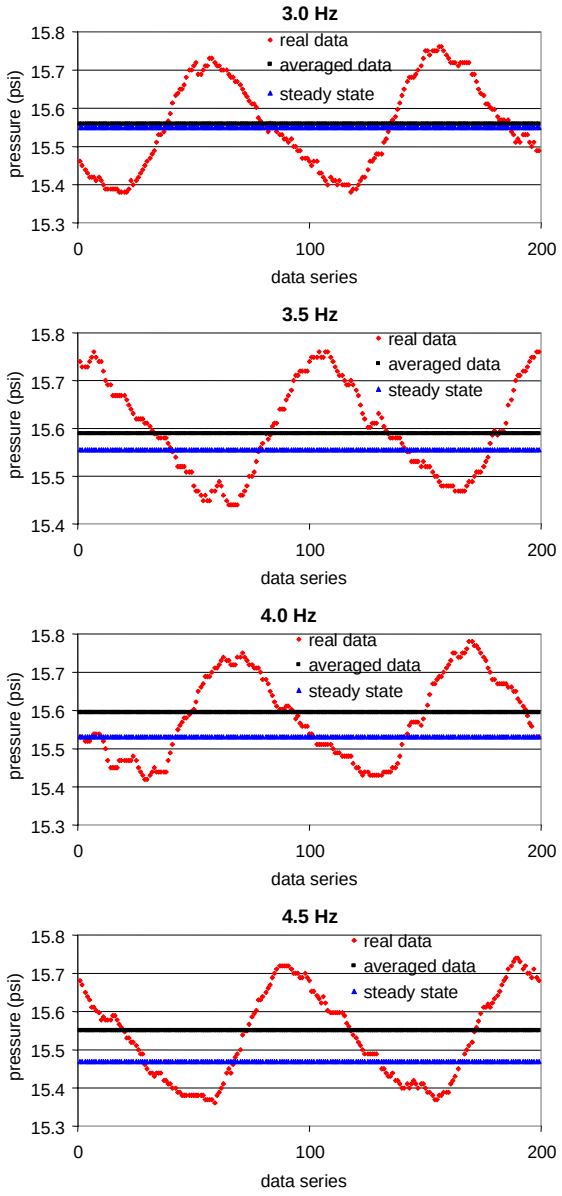

Figure 4.13: Downstream pressure under excitation (3.0 - 4.5 Hz, Berea sandstone).

Figure 4.14 illustrates the comparison of the downstream pressure under vibration with that at steady state for the Berea sandstone. The average downstream pressures at 1.0 Hz, 2.0 Hz and 2.5 Hz decreased compared to that at steady state. From 3.0 Hz to 4.5 Hz, the averaged value keeps increasing and reaches a maximum at 4.5 Hz. The different downstream pressure response at different vibration frequencies indicates that the effect of the excitation on the Berea sandstone is strongly dependent on the perturbation frequency.

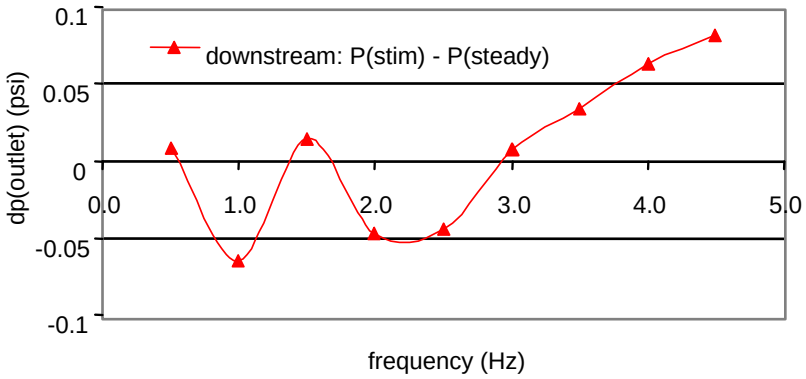

Figure 4.14: Downstream pressure vs. excitation frequency (Berea sandstone).

From the effect of vibration on downstream pressure, the excitation demonstrates positive effect on the ceramic core under 0.2 Hz to 5.0 Hz excitation. For the Berea sandstone, stimulation produces positive effect for frequencies higher than 3.0 Hz.

4.2.3. Differential Pressure Variation under Stimulation

Figure 4.15 shows the deviation of differential pressure under excitation from that at steady state for the ceramic core sample. The differential pressure under excitation is smaller than at steady state at all of the studied frequencies. Therefore, the vibration has a positive effect on the flow. The maximum difference was observed at 1.5 Hz, which indicates that the vibration has maximum positive effect on the ceramic core plug under this frequency. The variation of the curve reveals that the vibration effect is dependent on the frequency.

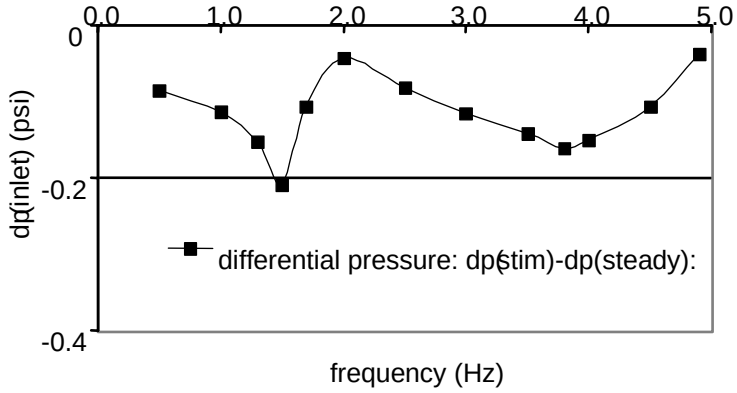

Figure 4.15: Differential pressure vs. vibration frequency (ceramic core).

Differential pressures in the Berea sandstone are shown in Figure 4.16. Distinct from the ceramic core, the difference between the differential pressure under vibration and that at

steady state does not show values consistently smaller than zero under all investigated frequencies. The difference is greater than zero from 0.5 Hz to 3.0 Hz. This illustrates that the excitation increases the pressure drop in the Berea sandstone. In other words, the resistance to flow in the Berea sand is increased at these frequencies. At frequencies greater than 3.5 Hz, the excitation produces positive effect on the flow.

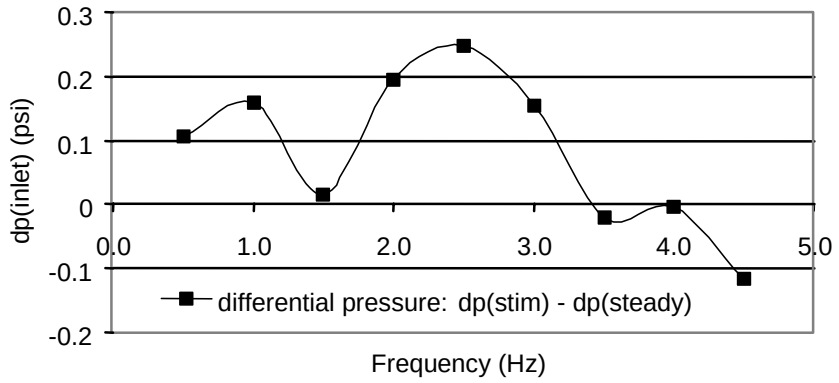

Figure 4.16: Differential pressure vs. vibration frequency (Berea sandstone).

The differential pressure variation under stimulation agrees with the response of upstream and downstream pressure in the two core samples. Differential pressure change verifies that the vibration reduced the flow resistance in the ceramic core over the entire vibration frequency range tested. However for the Berea sandstone, the vibration has positive effect only for frequencies greater than 3.0 Hz.

4.3. Phase Shift

Phase shift refers to the phase difference between the pressure signals at the two ends of the core. In steady-state flow, the phase shift between the inlet and outlet pressures is constant (and zero). Under vibration, the flow may change. Consequently the phase of the two pressure signals will not be constant or zero. Therefore phase interpretation is another useful way to evaluate the effect of excitation on flow.

Phase shift is a function of the perturbation signal frequency, wave type, properties of the medium through which the wave signal propagates, and the geometric characteristics of the medium. For different wave types in different porous media, the phase shift is

generally different. Consequently, phase delay analysis can be helpful to evaluate the physical, chemical, or geometrical properties of the porous medium.

When fluids flow in a porous medium, to overcome the friction acting on the interface of the solid and liquid phases, the pressure will decline along direction of flow. This results in pressure magnitude attenuation and phase distortion. In geophysics, the phase distortion is attributed to the effect of a slow wave, which is a property of the solid matrix.

The flow rate, injecting pressure and the local properties of the porous medium are constant under steady state injection. Therefore the solid phase is in a static state. The solid matrix is compressed while the solid particles remain motionless. There is no variation of the geometric shape of the channel or pore spaces. Because there is no external interference signal, the phase of the pressure signal is constant. The macroscopic phase delay between two ends of the rock remains constant with time under steady flooding.

Under vibration conditions, pressure perturbation in the fluid induces local geometric property variation in the solid phase and the friction changes along the interface between the fluid and solid phases. Two kinds of wave coexist under excitation conditions and each propagates predominantly in different media. The compression wave propagates mainly in the fluid phase while the shear wave propagates mainly in the solid matrix. Unlike in steady-state conditions, the macroscopic phase delay in the core sample in the fluid phase will be dominated by both compression wave (in fluid phase) and shear wave (in solid matrix). At the microscopic scale, the propagation of the shear wave has an effect on the inner friction between the fluid phase and solid phase and oscillation of the solid particles along the inner boundary of the channels and pore spaces. The interphase friction and the solid particle oscillation have dominant effects on the pressure attenuation and phase shift in the fluid phase. Consequently, the phase delay will be different from the phase response under steady flow.

For excitation in multiphase flow, the situation will be more complicated because of the complex properties of fluids and interaction between fluids. The interpretation of the stimulation mechanism should couple the multiple phase motions. No promising model has been established yet.

4.3.1. Phase Delay in the Experiments

Plotting the upstream and downstream pressures on the same plot can demonstrate the phase shift. This method visualizes the phase delay directly, and makes it easy to interpret the phase shift quantitatively.

The phase shift in the ceramic core sample as a function of frequency is illustrated in Figures 4.17 – 4.18. The phase delay keeps increasing with the excitation frequency. The phase variation is approximately constant at 40 degrees, at frequencies below 0.8 Hz. From 0.8 Hz to 1.5 Hz, the phase shift jumped to 68 degrees, and recoiled back to 55 degrees with frequency increasing to 2.0 Hz, dropped further to 50 degrees and stayed constant from 2.5 Hz to 5.0 Hz. The apparent deviation of phase delay at 1.5 Hz demonstrates that something happened in the porous medium due to the vibration. This observation is consistent with the differential pressure response.

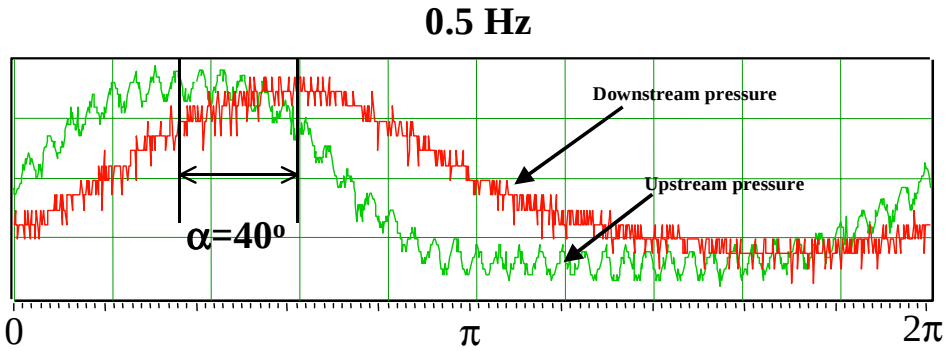

Figure 4.17: Phase shift under vibration (0.5 Hz, ceramic core).

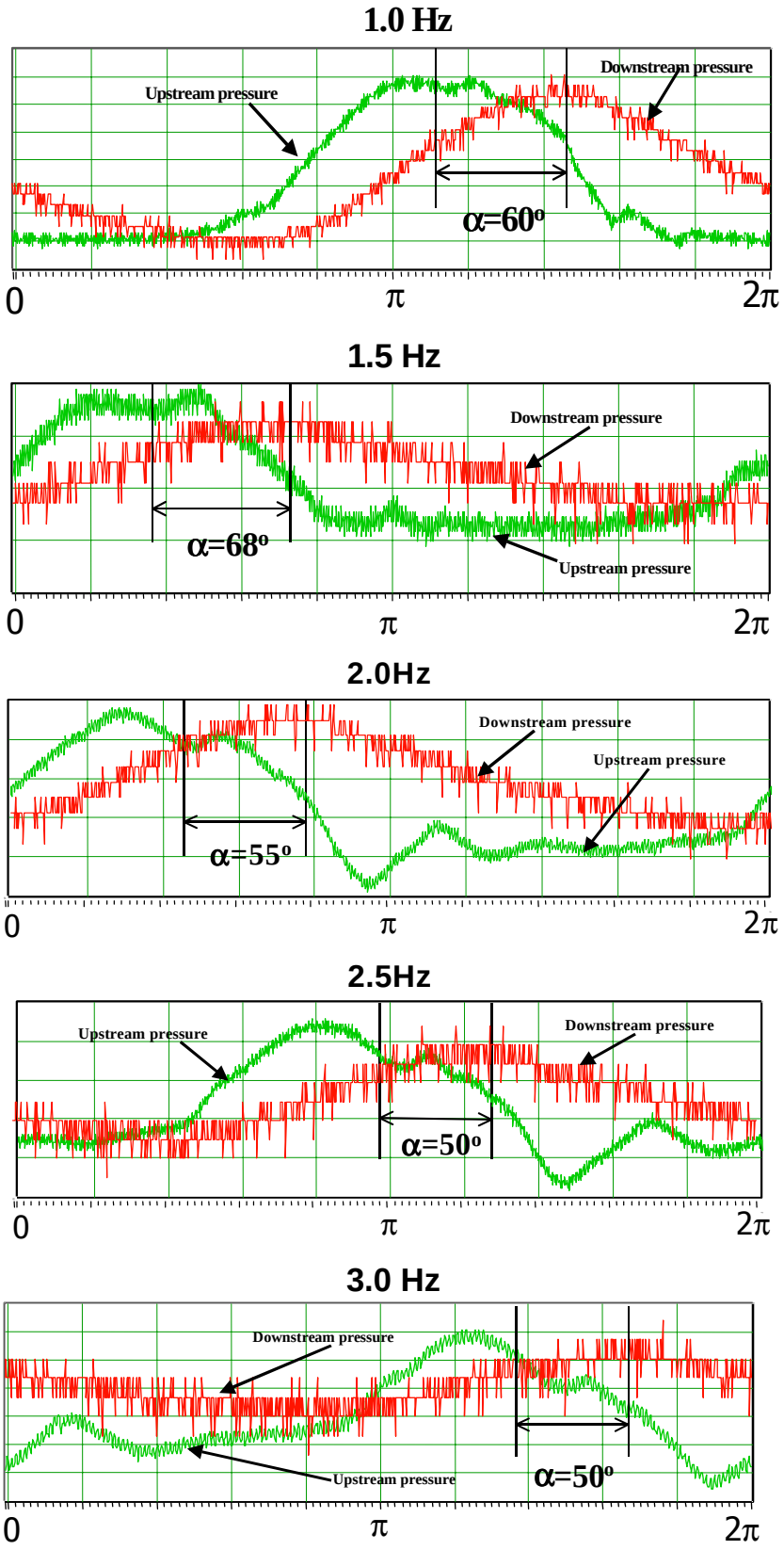

Figure 4.18: Phase shift under vibration (1.0 – 3.0 Hz, ceramic core).

The phase shift for the Berea sandstone is shown in Figures 4.19 – 4.20. Unlike in the ceramic core, the phase shift in Berea sandstone increased continuously with frequency. At very low frequency, the phase delay was smaller than the phase shift of the ceramic core. From 0.2 Hz to 1.5 Hz, the phase shift increased at approximately the same rate in the two samples. Beyond 1.5 Hz, the two responses demonstrated definitely different character.

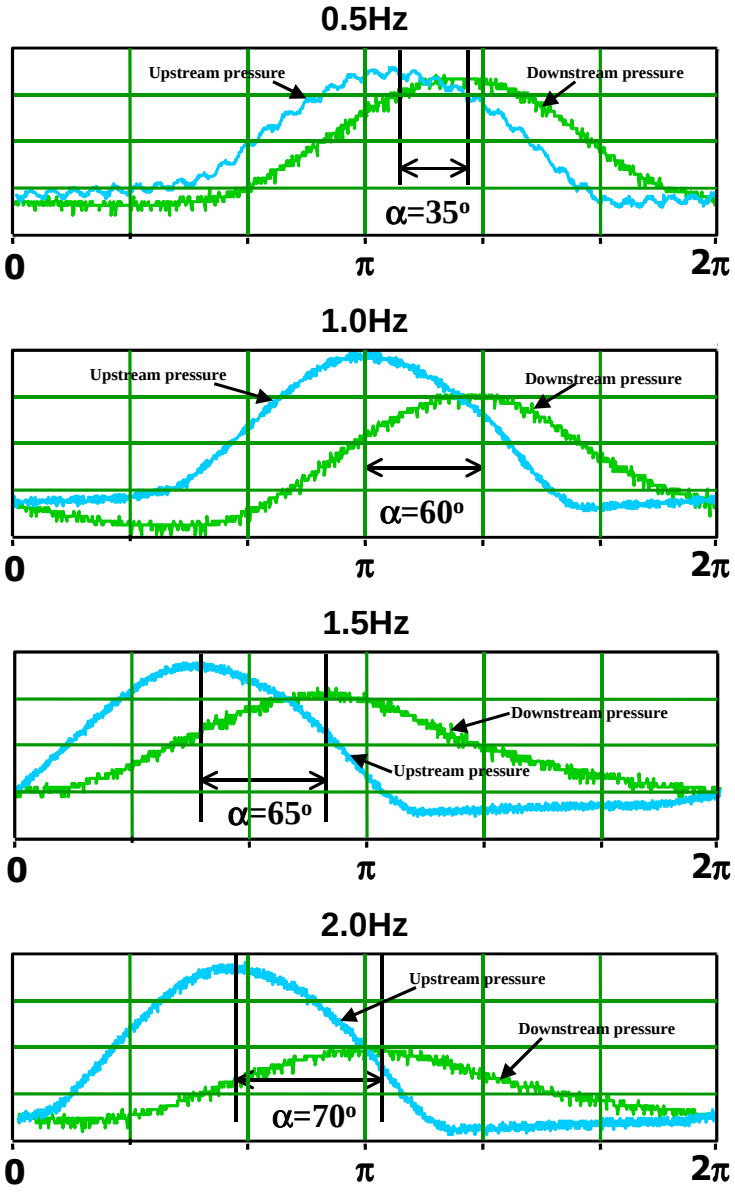

Figure 4.19: Phase shift under vibration (0.5 - 2.0 Hz, Berea sandstone).

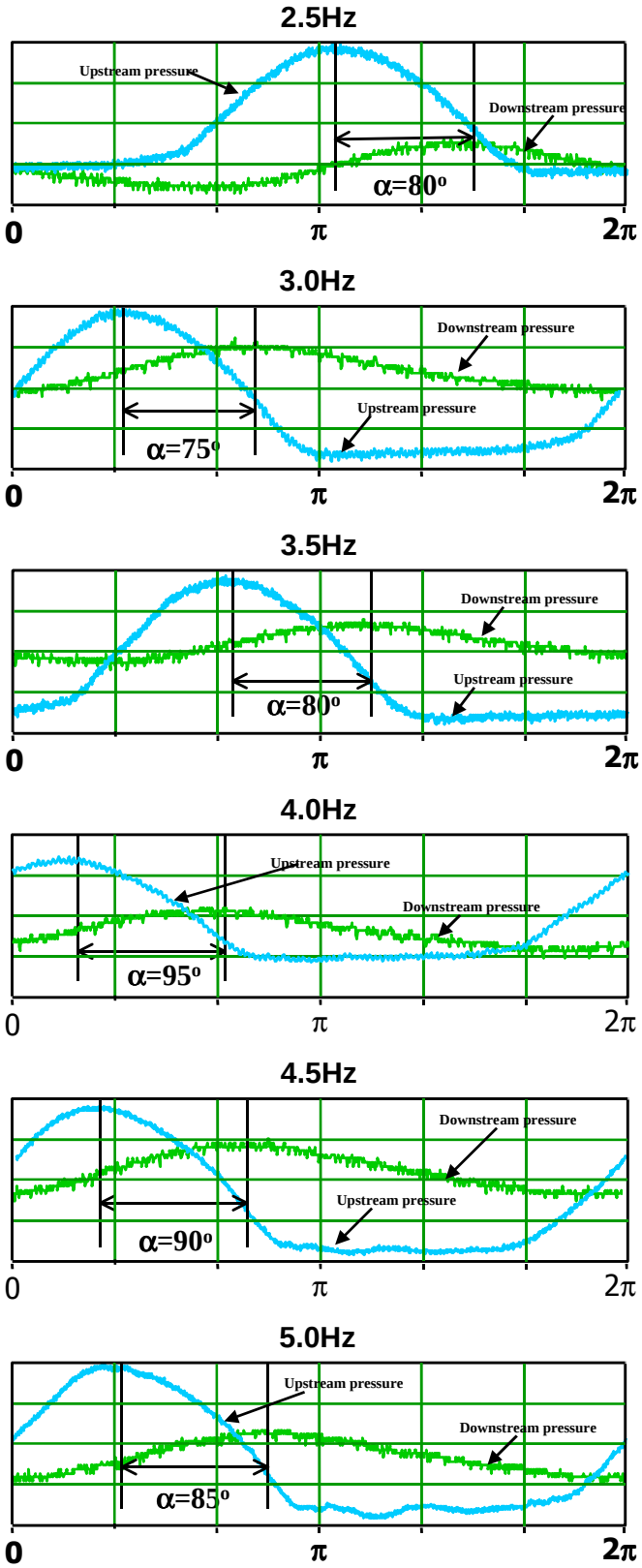

Figure 4.20: Phase shift under vibration (2.5 - 5.0 Hz, Berea sandstone).

Figure 4.21 illustrates the phase shift of the ceramic core quantitatively under different vibration frequencies. This figure verifies that 1.5 Hz is an interesting point, which needs detailed study. The phase delay versus frequency in the Berea sandstone is shown in Figure 4.22. The phase shift increases with frequency, except for slight decreases at 2.5 Hz and 4.0 Hz. The phase delay response is different from the ceramic core, and the plot verifies that the 2.5 Hz and 4.0 Hz observations need careful study.

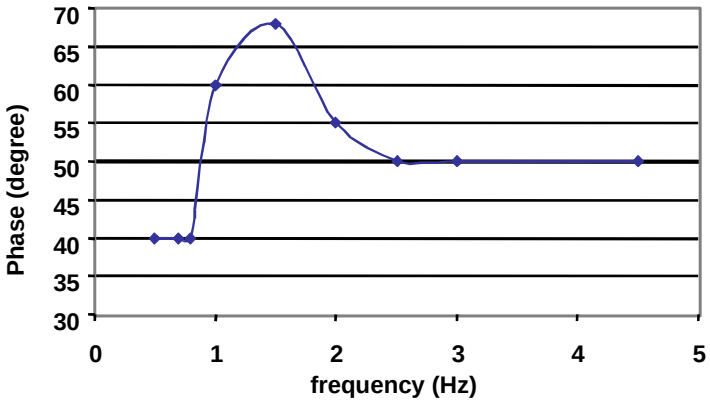

Figure 4.21: Phase delay vs. excitation frequency (ceramic core).

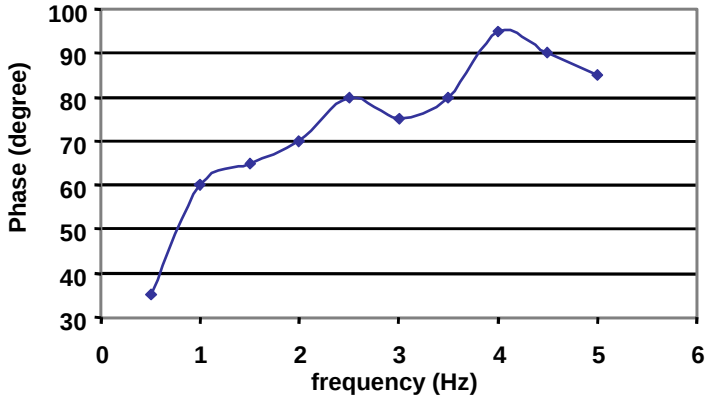

Figure 4.22: Phase delay vs. excitation frequency (Berea sandstone).

Another method to interpret the phase shift under excitation is from the p_{in} vs. p_{out} cross-plot. The pressure perturbation signal followed a sine-wave shape. Due to the phase delay, the p_{in} vs. p_{out} cross-plot will be an ellipse. Figure 4.23 shows this idea. The angle ***beta*** represents the phase delay of the pressure signals at the two ends of the rock sample. With the inlet pressure coming down the summit of the sine wave, the outlet pressure is still going up. As the inlet pressure decreases to some value, the downstream pressure reaches the maximum. So angle ***beta*** is always read from $p_{in}(max)$ to $p_{out}(max)$ or from

p_{in}(min) to ***p_{out}(min)***. If the phase delay is beyond 2π (which could be possible in reality), the downstream signal is out of phase, but this can not be shown on the ***p_{in}*** vs. ***p_{out}*** cross-plot.

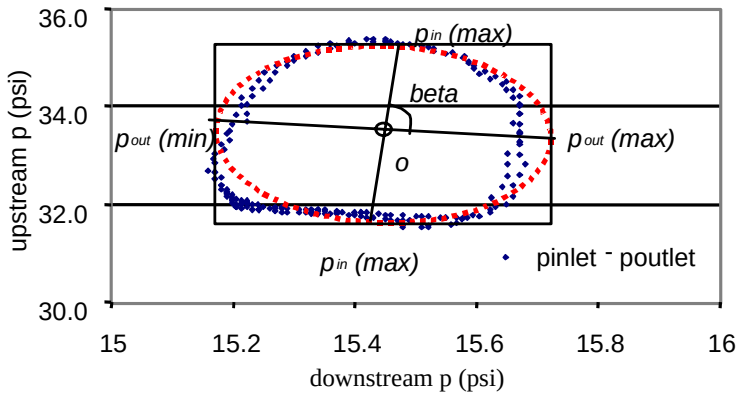

Figure 4.23: Phase delay interpretation at 1.5 Hz excitation (Berea sandstone), measured data and fitted ellipse

The disadvantage of phase delay analysis from the ***p_{in}*** vs. ***p_{out}*** cross-plot is the loss of pressure magnitude information. The plot is in Cartesian coordinates; the angle value may be difficult to read. To determine ***beta***, one has to determine the pair of peak values: ***p_{in}(min)***, ***p_{out}(min)*** or ***p_{in}(max)***, ***p_{out}(max)*** first. Data ambiguity sometime complicates the identification of the peak points. Consequently, the ***p_{in}*** vs. ***p_{out}*** cross-plot shows the magnitude of phase delay only roughly.

For the ceramic core plug, the upstream pressure versus downstream pressure plots in Figures 4.24 – 4.25 illustrate the phase angle change under different frequencies. However the pressure signal is rather noisy and the pressure ellipse is hard to determine.

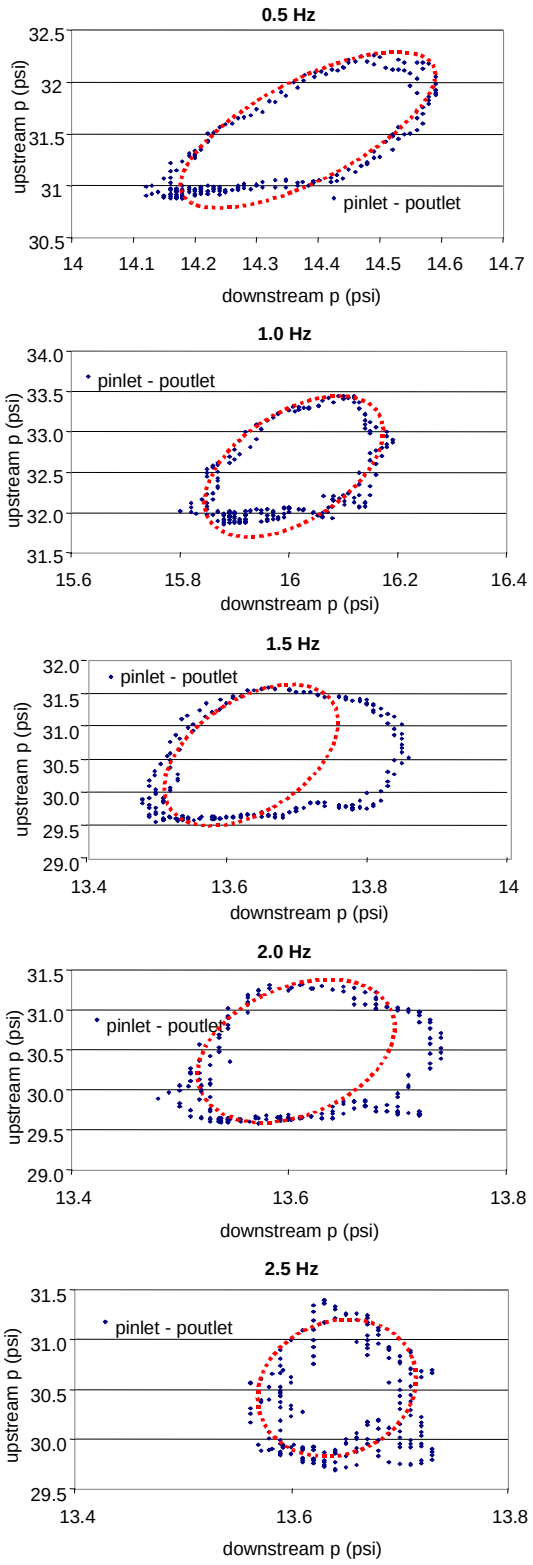

Figure 4.24: Upstream pressure vs. downstream pressure (0.5 – 2.5 Hz, ceramic core).

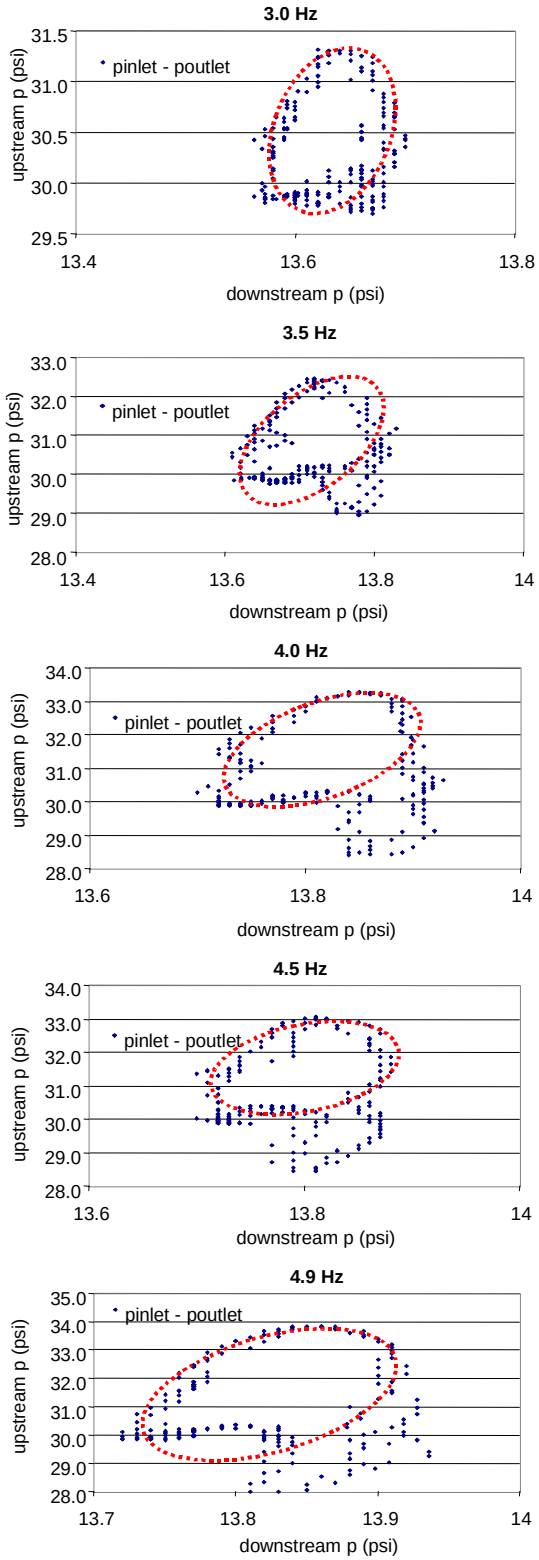

Figure 4.25: Upstream pressure vs. downstream pressure (3.0 – 4.9 Hz, ceramic core).

Figures 4.26 - 27 show the p_{in} vs. p_{out} plot for the Berea sandstone. The pressure signal for Berea sandstone is smoother than that for the ceramic core and the pressure ellipse is

easier to identify. The rotation of the ellipse under different frequencies clearly reveals the phase shift under different excitation conditions.

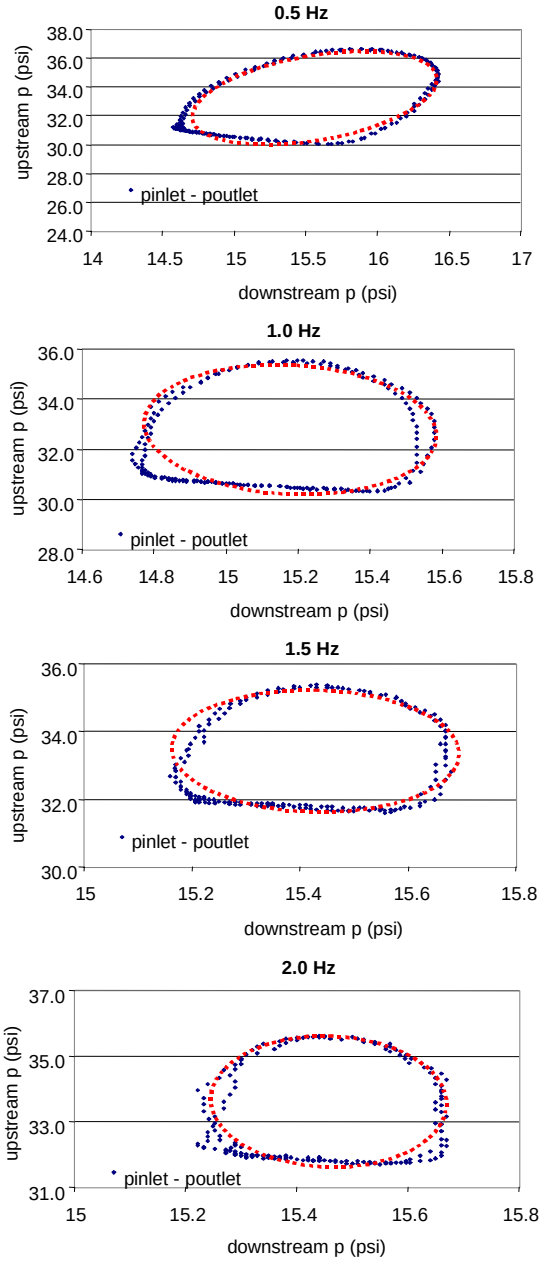

Figure 4.26: Upstream pressure vs. downstream pressure (0.5 – 2.0 Hz, Berea sandstone).

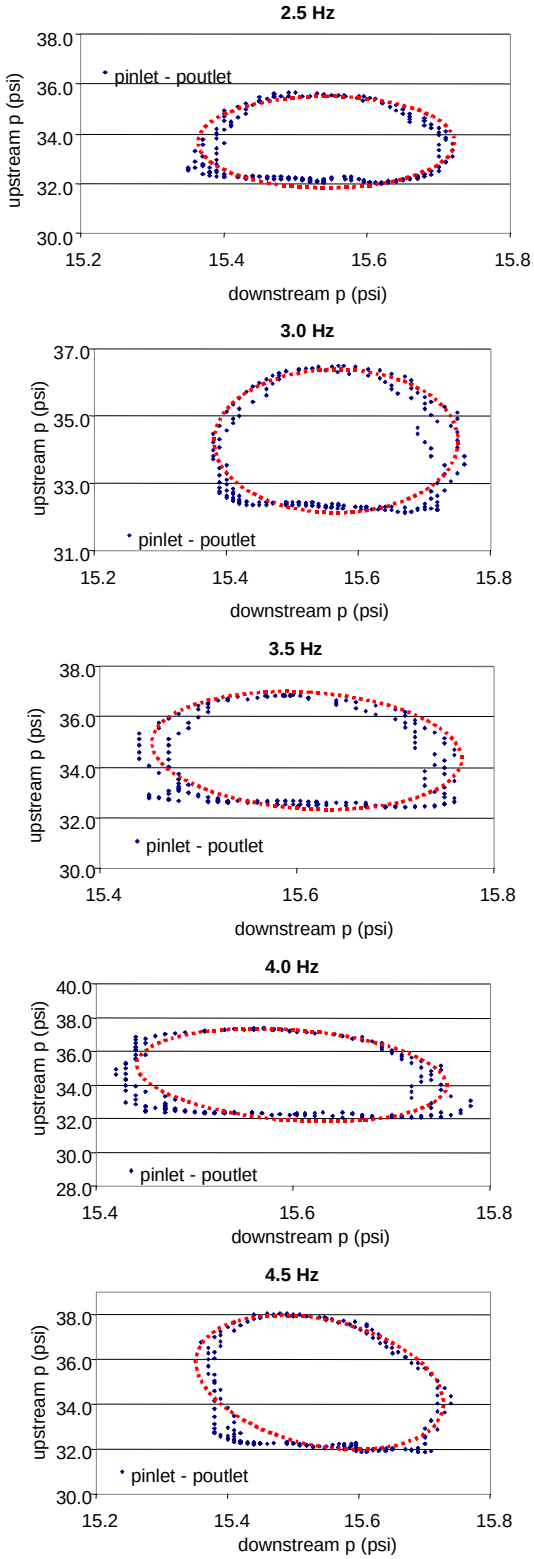

Figure 4.27: Upstream pressure vs. downstream pressure (2.5 – 4.5 Hz, Berea sandstone).

4.4. Differential Pressure versus Vibration Intensity

The apparently different phase response and differential pressure variation at some specific frequencies revealed that detailed study at those specific frequencies was necessary. The ceramic core was chosen for this purpose.

The deviation of differential pressure and phase delay from the normal track for the ceramic sample at 1.5 Hz demonstrates that the 1.5 Hz is a critical point that is distinct from other frequencies. To investigate the difference, three frequencies, 1.0 Hz, 1.5 Hz and 2.0 Hz, were selected and examined. Figures 4.28 – 4.30 show the upstream and downstream pressure variation from steady state for 1.0 Hz, 1.5 Hz and 2.0 Hz respectively. The 1.0 Hz and 2.0 Hz pressure responses show the same characteristic (the deviation is greater than zero and keeps increasing with rising intensity), which is apparently different from the random character demonstrated at 1.5 Hz excitation.

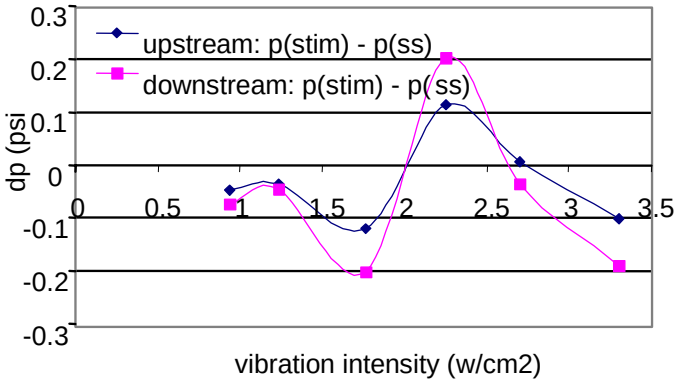

Figure 4.28: Upstream and downstream pressure vs. vibration intensity (1.5 Hz, ceramic core).

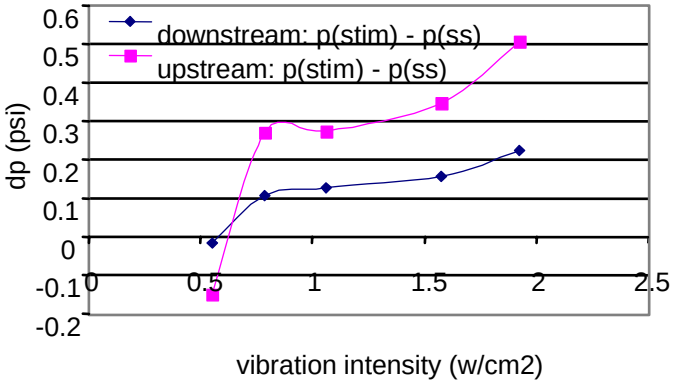

Figure 4.29: Upstream and downstream pressure vs. vibration intensity (1.0 Hz, ceramic core).

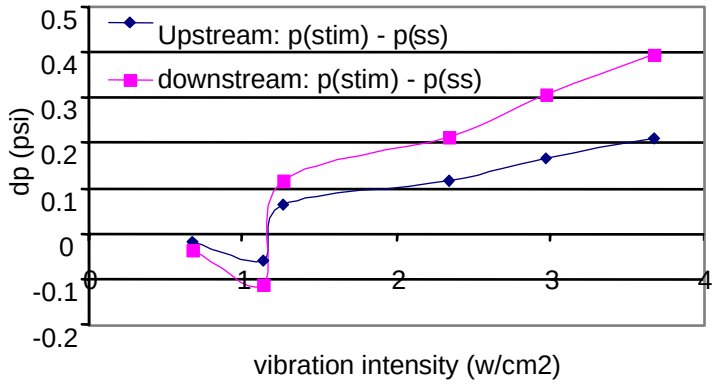

Figure 4.30: Upstream and downstream pressure vs. vibration intensity (2.0 Hz, ceramic core).

Figures 4.31 – 4.33 show the differential pressure change at the three frequencies. The differential pressure under 1.5 Hz vibration is lower than at steady state and keeps decreasing with increasing stimulation intensity, which means the vibration has a positive effect on flow. The 1.0 Hz and 2.0 Hz responses show a different trend, the differential pressure at these two frequencies is greater than at steady state and keeps increasing with the excitation intensity. Therefore the vibration at 1.0 Hz and 2.0 Hz increased the flow resistance in the porous medium.

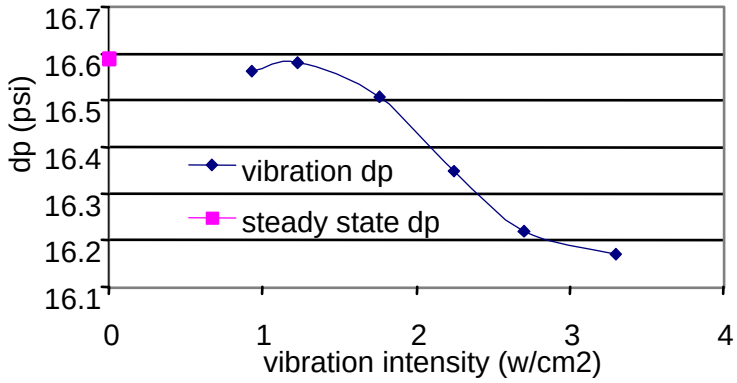

Figure 4.31: Differential pressure vs. vibration intensity (1.5 Hz, ceramic core).

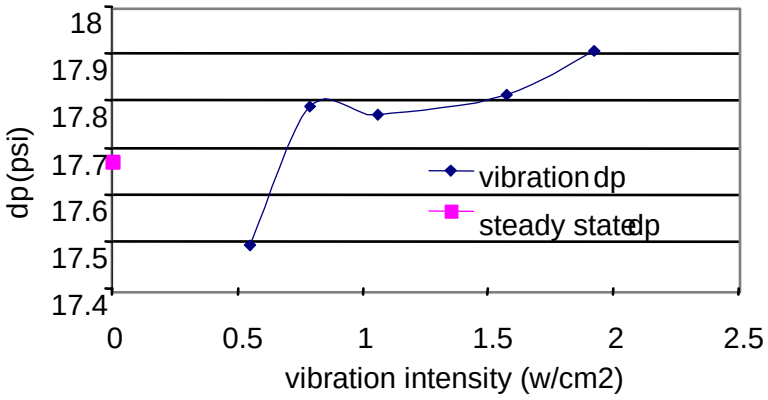

Figure 4.32: Differential pressure vs. vibration intensity (1.0 Hz, ceramic core).

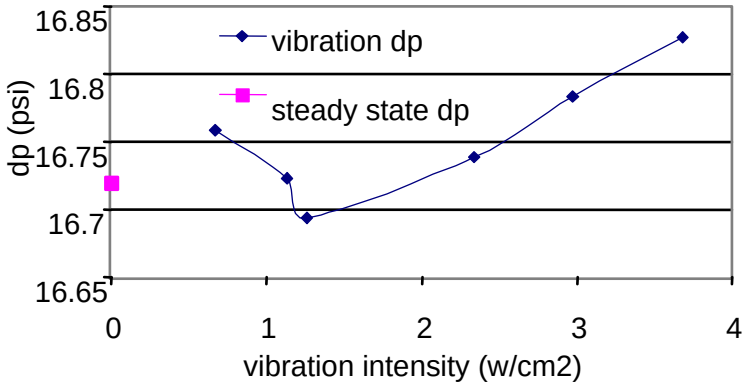

Figure 4.33: Differential pressure vs. vibration intensity (2.0 Hz, Ceramic core).

The upstream, downstream and differential pressure responses under different stimulation intensity verify that the excitation effect on the ceramic core is independent of the stimulation intensity. Therefore the vibration effect under our current observation is dominated only by the vibration frequency.

4.5. Discussion

Under excitation, the dynamic permeability of the rock will be used to describe the flow. The traditional static parameters are insufficient to characterize the dynamic problem. The dynamic permeability of the rock matrix is dominated by the coupling of the solid and fluid motion. Under excitation, motion of the solid phase at the interface of the tortuous channels or pore spaces will affect the flow. The solid particles along the interface of the channels and pore spaces will be activated and will oscillate under the perturbation of the injecting pressure. Consequently, the interaction of the solid and liquid phase will be different than at steady state, and the dynamic viscosity of fluid is not appropriate under

this condition. For elastic solid systems, the geometric shape of the pore spaces can change under resonant excitation. Darcy's law, which is commonly used to describe the steady state flow, is no longer valid. The mobilization of in-situ clay fines is another contribution to the variation of the permeability. All of these factors, which are ignored under steady-state injection, will contribute to the stimulation or reduction of flow.

In this study, the magnitude of upstream, downstream and differential pressures, compared with those at steady state reveal that the excitation has some positive effects both on the ceramic core plug and on Berea sandstone. Also, the different pressure responses of the ceramic core and Berea sandstone emphasize the complexity of the elastic wave effect on porous media with different physical properties.

Based on the apparent phase shift, but small magnitude pressure variation in our laboratory results, we believe that the vibration responses on the Berea sandstone and ceramic core are caused by weak waves, which form in the rock matrix, and by the change in dynamic viscosity in the fluid phase. For the ceramic core plug, the differential pressure remains lower than during steady injection (Figure 4.15). Small magnitude excitation seems unlikely to induce solid particles to vibrate in the ceramic matrix. Therefore, the differential pressure decrease under excitation may be caused by dynamic viscosity decrease in the fluid phase. For the Berea sandstone, the differential pressure change reveals distinct properties under different frequencies (Figure 4.16). At frequencies below 3.5 Hz, the differential pressure increases, which indicates a negative effect of the vibration. For frequencies greater than 3.5 Hz, the differential pressure is lower than at steady state. Therefore the excitation affects the flow positively. This distinct response gives the hint that weak elastic waves exist in the Berea sand matrix. The weak waves in the solid phase couple with the compression wave in the fluid phase. The combined action could cause the waves in the different phases to reinforce or counteract each other, as suggested by the theoretical work of Pan (1999). At macroscopic scale, the pressure drop in the rock may increase under some frequencies, and decrease under others.

Grain size is an important parameter in evaluating the effect of vibration on the flow. Generally, for porous media formed by fine grains, the dimension of the channels or pore spaces is relative small, and the inner space of the pores is rougher compared to porous media composed of coarse grains. The dominating effect of dynamic viscosity will be stronger, and harmonic vibration of the fluid in the pore spaces is relatively difficult to realize. The vibration effect might be viscosity-dominated. For porous media constructed of coarse particles, the inner space of the channels or pores is larger; harmonic vibration in the fluid phase is relatively easier to generate in the pore spaces. Therefore the stimulation effect might be determined by the join action of dynamic viscosity change and harmonic wave covibration in the pore spaces. For the two core samples in this study, the vibration effect on the ceramic core might be dynamic viscosity determined. As for the Berea sandstone, the effect might be dominated by the combined effect of the dynamic viscosity change and harmonic wave propagation.

One more point that needs to be noted is that the vibration effects on both the ceramic and Berea sandstone demonstrate frequency dependence. Figures 4.4 and 4.7 show the variation of the upstream pressure. Figures 4.11 and 4.14 illustrate the change of downstream pressure. Figures 4.15 and 4.16 verify the differential pressure change for the two samples respectively. The fluctuation of the upstream, downstream pressure and differential pressure under excitation implies that these three pressure variations are frequency-dependent. Under some specific frequencies, the vibration produces strong positive effect.

Currently, only two rocks with different physical properties have been studied. Even though some intriguing phenomena have been observed in our laboratory, more rock samples with different physical properties need to be studied before drawing any convincing conclusions. Also, the interesting vibration response of the ceramic and Berea sand samples only tell us that the elastic wave vibration does appear to affect the flow properties of the porous media, and further studies are necessary.

Chapter 5

5. Conclusions and Suggestions

5.1. Conclusions

1. The response to vibration in the fluid-phase demonstrated small positive effect on the single-phase flow system at some specific frequencies.

2. Differential pressure variation and phase shift behaviors were not the same in the ceramic core and in the Berea sandstone, which indicates the flow property changes were different in different porous media.

3. Upstream, downstream and differential pressure variation versus intensity showed that the pressure response is independent of the vibration intensity. Pressure change under excitation depended only on the vibration frequency in our current observations.

4. The apparent phase shift and low magnitude differential pressure decrease compared with those at steady state for the ceramic core may suggest a dynamic viscosity change under excitation.

5. Distinct differential pressure response under different frequencies for the Berea sandstone may suggest that weak waves were induced in the solid matrix during excitation. Under some specific frequencies, the excitation has positive effect on the flow.

6. Grain size should be an important parameter in defining the vibration effect on single-phase flow. For porous media formed by fine grains, the vibration effect may be determined by the dynamic viscosity change. For porous media composed of coarse

particles, the excitation response may be dominated by the joint effect of the dynamic viscosity change and elastic waves.

5.2. Suggestions for Future Work

1. Expand the capacity of the current experiment by running at higher frequency, with higher injection pressure vibration.

2. Monitor the in-situ motions in liquid and solid phases. The elastic excitation works prominently on the local pore spaces; therefore, monitoring the in-situ solid and fluid properties accurately would provide more valuable information to interpret the effect of elastic vibration.

3. Excite a loose sand pack; test the effect of oscillation in the solid phase on stimulation. Tight sandstone is hard to vibrate by stimulating the fluid phase. The energy transmission efficiency in the fluid phase is much lower than in the solid phase, and the wave amplitude attenuation in the fluid phase increases with frequency. Therefore, vibrating a loose sand pack would be a useful method to interpret the elastic wave stimulation effect.

4. Stimulation in multiphase flow. This is much more like the field situation. Also, multiphase vibration can include the elastic wave effect on water-oil ratio, relative permeability variation, and the interaction among fluid phases, which would be more interesting to field cases.

5. Excite the solid matrix rather than vibrating the fluid phase.

Nomenclature

w	vertical solid displacement
t	time
l	characteristic length at pore scale
L	characteristic length at macroscopic scale
$\langle u \rangle_p$	volume-averaged fluid velocity over the pore space
yl	initial half channel width at pore scale
xl	channel length at pore scale
p	pore pressure
X, Y	spatial variables at the macroscopic scale
k	effective permeability
v_p	p – wave propagation velocity in the solid
S	channel width at pore scale
D_{piston}	diameter of pump piston (mm)
l_{max}	maximum stroke of the pump piston (mm)
c_w	water compressibility (psi^{-1})
v	total volume in the injection system (ml)
d_{piston}	diameter of cylinder piston (mm)
f_{mass}	mass force (kg)
f_{force}	force (N)

Symbols

ε	Length ration of the pore scale and the macroscopic scale, $\varepsilon = l/\boldsymbol{L}$
λ	Lamé parameter

ρ_f fluid density

μ fluid viscosity

ϕ effective porosity

ρ_s solid density

Subscripts

p pore space

s solid space

References

[1] Abousleiman, Y, Cheng A. H-D., Jiang , C., and Roegiers, J.-C.: "Poroviscoelastic Analysis of Borehole and Cylinder Problems," *Acta Mechanica* (1996) 119, No. 1-4, 199-219.

[2] Amaefule, J. O., Wolfe, K., Ajufo, A. O. and Peterson, E.: "Laboratory Determination of Effective Liquid Permeability in Low-Quality Reservoir Rocks by the Pressure Pulse Technique," paper *SPE 15149* presented at 56th California Regional Meeting of the Society of Petroleum Engineers, Oakland, April 1986.

[3] Auriault, J.-L.: "Heterogeneous Medium. Is an Equivalent Macroscopic Description Possible? " *International Journal of Engineering Sciences* (1991) 29, No. 7, 785-795.

[4] Auriault J. L.: "Deformable Porous Media with Double Porosity. Quasi-Statics. I: Coupling Effects," *Transport in Porous Media* (1992) 7, 63-82.

[5] Beresnev, I. A. and Johnson, P. A.: "Elastic-Wave Stimulation of Oil Production: A Review of Methods and Results," *Geophysics* (June 1994) 59, No. 6, 1000-1017.

[6] Bernabe, Y.: "The Frequency Dependence of Harmonic Fluid Flow Through Networks of Cracks and Pores," *PAGEOPH* (1997) 147, No. 3, 489-506.

[7] Biot, M. A.: "Theory of Propagation of Elastic Waves in a Fluid Saturated Porous Solid," *Journal of Acoustical Society of America* (March 1956) 28, No. 2,168-191.

[8] Birch, F.: "Compressibility; Elastic Constants," *Handbook of Physical Constants*, (1966) 97, 97-174.

[9] Bonnet, G.: "Basic Singular Solution for a Poroelastic Medium in the Dynamic Range," *Journal of Acoustical Society of America* (November 1987) 82, No. 5, 1758-1762.

[10] Brace, W. F., Walsh, J. B. and Franges, W. T.: "Permeability of Granite Under High Pressure," *Journal of Geophysics Research* (March 1968) 73, 2225-36.

[11] Bredehoeft, J. D.: "Response of Well-Aquifer Systems to Earth Tides," *Journal of Geophysical Research* (June 1967) 72(12).

[12] Brown, R. J. S.: "Connection Between Formation Factor for Electrical Resistivity and Fluid-solid Coupling Factor in Biot's Equation for Acoustic Waves in Fluid-filled Porous Media," *Geophysics* (1980) 45, 1269-1275.

[13] Bruce, G. H., Peaceman, D. W., Rachford, H. H. and Rice, J. D.: "Calculation of Unsteady-State Gas Flow Through Porous Media," *Journal of Petroleum Technology* (March 1953) 79-92, Trans. AIME (1953), 198.

[14] Chang, S. K., Liu, H. L. and Johnson D. L.: "Low-Frequency Tube Waves in Permeable Rocks," *Geophysics* (April 1988) Vol. 53, No. 4, 519-527.

[15] Charlaix, E., Kushnick, A. P., and Stokes, J. P.: "Experimental Study of Dynamic Permeability in Porous Media," *Physical Review Letters* (1988b) 61, No. 14, 1595{1598.

[16] Charlaix, E. and Gayvallet, H.: "Hydrodynamic Dispersion in Networks of Capillaries of Random Permeability," *Europhysics Letters* (September 1991) 16, No. 3, 259-264.

[17] Chen, T. and Stagg, P. W.: "Semilog Analysis of the Pulse-Decay Technique of Permeability Measurement," paper *SPE 11818*.

[18]Cherskiy, N. V., Tsarev, V. P., Konovalov, V. M., and Kusnetsov, O. L.: "The Effect of Ultrasound on Permeability of Rocks to Water," Transactions (Doklady) of the USSR Academy of Sciences, Earth Science Section (1977), 232, 201-204.

[19] Crosnier, B., Fras, G., and Jouanna, P.: "Reconnaissance of Fractured Media with Several Systems of Fractures by Means of Harmonic Techniques," *Rock Mechanics and Rock Engineering* (1985) 18, 77-105.

[20] Dai, N., Vafidis, A., and Kanasewich, E. R.: "Wave Propagation in Heterogeneous Porous Media: A Velocity-Stress, Finite-Difference Method," *Geophysics* (March-April 1995) 60, No. 2, 327-339.

[21] Dean et al.: "A New Method to Monitor Compaction and Compressibility Changes in Offshore Chalk Reservoir by Measuring Formation Pressure Variation Caused by the Sea Tide," paper *SPE 23142* presented at 1991 Offshore Europe Conference, Aberdeen.

[22] Depollier, C., Allard, J. F., and Lauriks, W.: "Biot Theory and Stress-Strain Equations in Porous Sound-Absorbing Materials" *Journal of Acoustical Society of America* (December 1988) 84, No. 6, 2277-2279.

[23] Deresiewicz, H. and Rice, J. T.: "The Effect of Boundaries on Wave Propagation in a Liquid Filled Porous Solid," *Bulletin of Seismology Society of America* (1962) Vol. 52, 595.

[24] Duhon, R. D., "*An Investigation of the Effect of Ultrasonic Energy on the Flow of Fluids in Porous Media*," presented as a dissertation for the Degree of Doctor of Philosophy, University of Oklahoma (1964).

[25] Dusseault, M. Davidson, B. and Spanos, T.: "Pressure Pulsing: The Ups and Downs of a Starting a New Technology," *Journal of Canadian Petroleum Technology* (2000) 39, No. 4.

[26] Dyblenko, V. P., Tufanov, I. A., Suleymanov, G. A., and Lysenkov, A. P.: "Percolation Phenomena and Processes in Saturated Porous Media under the Vibro-Wave Action, in Ways of Intensification of Oil Production," Proc. (Trudy) Bashkir Research and Design Institute of Oil (1989): 45-51 (in Russian).

[27] Fatt, I.: "A Demonstration of the Effect of 'Dead-End' Volume on Pressure Transients in Porous Media," *Trans.*, AIME (1959) Vol. 216, 449-454.

[28] Forchheimer, P. F.: "Wasserbewegung durch Boden," *Zeitschrift des Vereines deutscher Ingenieure* (1901) 45, No.5, 1781-1788.

[29] Foster, W. R., McMillen, J. M., and Wallick, G. C.: "The Equations of Motion of Fluids in Porous Media: II. Shape of Pressure Pulses," paper *SPE 2322* presented at the 1968 SPE Annual Meeting.

[30] Freeman, D. L. and Bush, D. C.: "Low-Permeability Laboratory Measurements by Nonsteady-State and Conventional Methods," *SPE 10075, Society of Petroleum Engineering Journal*, 1983.

[31] Hamilton, M. F.: "Fundamentals and Applications of Nonlinear Acoustics," *Nonlinear Wave Propagation in Mechanics –AMD-77*, America Society of Mechanical Engineering, New York. (1986).

[32] Hassanzadeh, S.: "Acoustic Modeling in Fluid Saturated Porous Media," *Geophysics* (1991) 56, 424-435.

[33] Haskett, S. E., Narahara, G. W. and Holditch, S. A.: "A Method for the Simultaneous Determination of Permeability and Porosity in Low-Permeability Cores," paper *SPE 15379* presented at the 1986 annual meeting, New Orleans.

[34] Johnson, P. A., Zinszner, B. and Rasolofosaon, P. N. J.: "Resonance and Elastic Phenomena in Rock," *Journal of Geophysical Research* (May 1996) Vol. 101, No. B5, 11553-11564.

[35] Johnson, P. A. and McCall, K. R.: "Observations and Implications of Nonlinear Elastic Wave Response in Rock," *Geophysics Research Letters* (1994) 21, 165-168.

[36] Klinkenberg, L. J.: "The Permeability of Porous Solids to Liquids and Gases," *Drill. & Prod. Prac.* (API 1941) 200.

[37]Kuznetsov, O. L., Vakhitov, G., and Simkin, E. M.: "Thousands Time Faster," *Technology and Science* (1986) No. 9, 12-13. (in Russian).

[38] Kouznetsov, O. L., Simkin, E. M., Chilingar, G. V. and Katz, S. A.: "Improve Oil Recovery by Application of Vibro-Energy to Waterflooded Sandstone," *Journal or Petroleum Science and Engineering* (1998) 19, 191-200.

[39] Li, L. P., Cederbaum, G., and Schulgasser, K.: “Vibration of Poroelastic Beams with Axial Diffusion,” *European Journal of Mechanics*, A: *Solids* (1996) 15, No. 6, 1077-1094.

[40] Medlin, W. L., Masse, L., and Zumwalt, G. L.: “Method for Recovery of Oil by Means of a Gas Drive Combined with Low Amplitude Seismic Excitation,” US Patent 4 417 621 (1983).

[41] Li, M. Y., Dong, Z. X., Ji, S. L., Wu, Z. L. and Zhao, L. Z.: “The Study of Oil Recovery by Water Flooding with Sound Vibration,” *Petroleum Science* (March 1999) Vol. 2 No. 1, 48.

[42] Nikolaevskiy, V. N.: “Mechanism and Dominant Frequencies of Vibrational Enhancement of Yield of Oil Pools,” Transactions (Doklady) of the USSR Academy of Science, Earth Science Sections (1989) 307, 570-575.

[43] Nikolaevskiy, V. N. et al.: “Residual Oil Reservoir Recovery with Seismic Vibration,” *SPE Production and Facilities* (May 1996).

[44] Norris, A. N.: “Radiation from a Point Source and Scattering Theory in a Fluid-Saturated Porous Medium,” *Journal of Acoustical Society of America* (1985) Vol. 77, 2012.

[45] Norris, A. N. and Grinfeld, M. A.: “Nonlinear Poroelasticity for a Layered Medium,” *Journal of Acoustical Society of America* (August 1995) 98, No. 2, 1138-1146.

[46] Odeh, A. S. and McMillen, J. M.: “Pulse Testing: Mathematical Analysis and Experimental Verification,” *Society of Petroleum Engineers Journal* (October 1972) 403-409.

[47] Ochs, D. E., Chen, H.-Y., and Teufel, L. W.: “Relating In-Situ Stress and Transient Pressure Testing for a Fractured Well,” Proceedings of the *SPE* Annual Technical Conference and Exhibition (October 1997) pt 1, 301-316.

[48] Oroveanu, T. and Pascal, K.: “On the Propagation of Pressure Waves in a Liquid Flowing Through a Porous Medium,” *Revue de Mechanique Applique* (1959) 4, No. 3, 445.

[49] Pan, Y.: "*Reservoir Analysis Using Intermediate Frequency Excitation*," presented as a dissertation for the Degree of Doctor of Philosophy, Stanford University (August 1999).

[50] Pinilla, J. F., Trevisan, O. V., and Tinoco, F. L.: "Coupling Reservoir and Geomechanics to Interpret Tidal Effects in a Well Test," *Proceedings of the 72nd Annual Technical Conference and Exhibition of SPE* (October 5-8 1997), 301-314.

[51] Sharma, A. and Roberts, P. M.: "Seismic Stimulation of Oil Production in Mature Reservoirs," *America Association of Petroleum and Geology Annual Convention, Extended Abstracts*, (1998). Vol. 2: A591.

[52] Sherborne, J. E.: "Recovery of Hydrocarbon," USA Patent 2 670 801 (1954).

[53] Simkin, E. M.: "Oil Will Return in Three Months," *Energy*, (1985) No.3, 44-47 (in Russian).

[54] Slattery, J. C.: "Flow of Viscoelastic Fluids Through Porous Media*" paper SPE 1684* (December 1966).

[55] Snarskiy, A. N.: "Determination of the Influence of Infrasonic Field on Oil Percolation Rate in Elementary Reservoir Model*," Transactions of the Higher School, Ser. Oil and Gas,* (1982) No. 1, 30-32.

[56] Stoll, R. D., and Bryan, G. M.: "Wave Attenuation in Saturated Sediments," *Journal of Acoustical Society of America* (1970) 47(5), 1440.

[57] Tencate J. A., Van Den Abeele, K. E. A., Shankland, T. J. and Johnson. P. A: "Laboratory Study of Linear and Nonlinear Elastic Pulse Propagation in Sandstone," *Journal of Acoustical Society of America* (September 1996). 1383-1391.

[58] Westermark, R. V., Brett, J. F. and Maloney, D. R.: "Enhanced Oil Recovery with Downhole Vibration Stimulation," *paper SPE 67303* (2001).

[59] Winkler, K. W., Nur, A.: "Seismic Attenuation: Effects of Pore Fluids and Frictional Sliding," *Geophysics* (January 1982) Vol. 47, 1-15.

[60]Winkler, .K. W., Liu, H. L. and Johnson D. L.: “Permeability and Borehole Stoneley Waves: Comparison Between Experiment and Theory,” *Geophysics* (January 1989) Vol. 54, 66-75.

[61] Zhu, X. and McMechan, G. A.: “Finite-Difference Modeling of the Seismic Response of Fluid-Saturated, Porous, Elastic Media Using Biot Theory,” *Geophysics* (1991) 56, 328-339.

[62] Zimmerman, C. and Stern, M.: “Analytical Solutions for Harmonic Wave Propagation in Poroelastic Media,” *Journal of Engineering Mechanics* (October 1994) 120, No. 10, 2154-2179.

[63] Zobnin, A. I., Kudryavtsev, B. A., and Parton, V. Z.: “Linearized Equations of Motion of a Viscous Fluid in a Porous Medium of Periodic Structure,” *Fluid Dynamics* (March-April 1988) 23, No. 2, 260-266.

[64] Zinov’yeva, G. P., Nesterov, I. I., Zdhakhin Y. L., Artma E. E., and Gorbunov Y. V.: “Investigation of Rock Deformation Properties in Terms of the Nonlinear Acoustic Parameter,” *Sov. Phys. Dokl., Science Section* (1989) 307, 337-341.

Appendix A

Derivation of Macroscopic Models after Pan (1999)

A porous medium with assumed periodical pore structure is adopted in deriving the five macroscopic models. Figure A.1 illustrates the basic sketch of the porous structure. The ratio of the period to the overall size of the porous medium, denoted by ε, which is a small number in Pan's asymptotic analysis. Generally the pore size is much smaller than the characteristic length of the reservoir. *P* in the Figure A.1 denotes pore space; *S* refers to solid matrix.

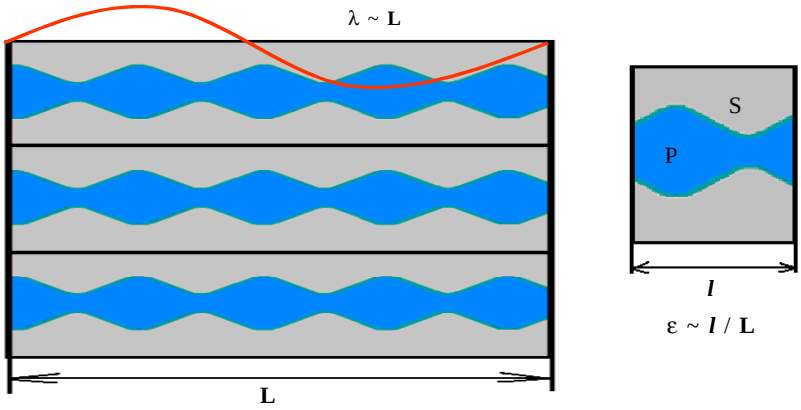

Figure A.1: Periodic porous medium.

Model 1: Acoustics of Empty Channels

For a porous medium filled with a very compressible and low viscosity fluid, the fluid can be ignored in studying the flow property of the porous system. The channel can be evaluated as empty channel vibrating under excitation.

In physical quantities, this model can be expressed as:

$$\frac{\partial^2 w}{\partial t^2} + O(\varepsilon) = 0 \qquad \textbf{(A-1)}$$

The perturbation to the solid is assumed to come from the oscillation of the fluid in the channel. The empty channel remains static if there is no perturbation.

Model 2: Acoustics of a Fluid in a Rigid Channel

For an incompressible fluid in a rigid channel, this model can be applied. Viscosity is the same order as in Model 1.

In physical quantities, the model can be written as:

$$\frac{\partial \langle u \rangle_p}{\partial X} + O(\varepsilon) = 0 \quad \textbf{(A-2)}$$

$$\frac{\partial \langle u \rangle_p}{\partial t} + \frac{3\mu}{\rho_f (yl)^2} \langle u \rangle_p = -\frac{\phi}{\rho_f} \cdot \frac{\partial p}{\partial X} + O(\varepsilon) \quad \textbf{(A-3)}$$

For steady state, Equation A-3 is Darcy's law for channel flow:

$$\langle u \rangle_p = -k \cdot \frac{\partial p}{\partial X} \quad \textbf{(A-4)}$$

Permeability is defined as:

$$k = \frac{\phi (yl)^2}{3\mu} \quad \textbf{(A-5)}$$

Model 3: Diphasic Macroscopic Behavior

This model introduces two macroscopic fields: the averaged fluid velocity and the averaged solid displacement, which are coupled together through the pore pressure and the channel width. The viscosity in this model is higher than in the previous two models, and the solid matrix is elastic.

In physical properties, this model can be defined as:

$$\frac{\partial^2 w}{\partial t^2} = -\frac{1}{\rho_s} \frac{\partial p}{\partial Y} + O(\varepsilon) \quad \textbf{(A-6)}$$

$$\frac{\partial \langle u \rangle_p}{\partial X} + \frac{1-\phi}{2} \frac{\partial}{\partial t} \left[\frac{\partial w}{\partial Y} + \frac{p}{\rho_s v_p^2} \right] + \frac{\phi}{S} \frac{\partial C_1}{\partial t} + O(\varepsilon) \quad \textbf{(A-7)}$$

$$\frac{\partial \langle u \rangle_p}{\partial t} + \left[\frac{6\mu}{\rho_f \cdot yl \cdot S} - \frac{19}{6S} \frac{\partial S}{\partial t} \right] \langle u \rangle_p = -\frac{\phi}{\rho_f} \frac{\partial p}{\partial X} + O(\varepsilon) \quad \textbf{(A-8)}$$

Model 4: Monophasic Elastic Behavior

For higher viscosity fluid or higher perturbation frequency, the porous media is dominated by monophasic behavior. The solid matrix is elastic.

The physical properties of the model is:

$$\frac{\partial w^2}{\partial t^2} = -\frac{1}{\phi\rho_s}\frac{\partial \langle p \rangle_p}{\partial Y} + O(\varepsilon) \quad \textbf{(A-9)}$$

$$\frac{1-\phi}{2}\frac{\partial}{\partial t}\left[\frac{\partial w}{\partial Y} + \frac{\langle p \rangle_p}{\phi\rho_s v_p^2}\right] + \frac{\phi}{S}\frac{\partial C_1}{\partial t} + \phi\frac{\partial C_u}{\partial X} + (\varepsilon) \quad \textbf{(A-10)}$$

Model 5: Monophasic Viscoelastic Behavior

For some very high viscosity fluids or high stimulation frequency, there will be no contrast between the mechanical properties of the materials in the porous medium. The solid and liquid phases will vibrate simultaneously. Therefore, the assumptions of negligible motions in the solid and liquid phases do not apply in this case. The solid and liquid phases will both participate in the horizontal and vertical oscillation. The general Navier–Stokes equation and elasticity equations at the pore scale have to be solved to derive the macroscopic description of the viscoelastic behavior.

Appendix B

Design of the Electromagnetic Exciter Stimulation System

The cost of the Electromagnetic Exciter and the Power Amplifier are functions of the output force and excitation amplitude. The physical requirement of the single-phase injection and reasonable flooding parameters were considered to design a laboratory-scale apparatus. A rigorous procedure for power-matching checking is necessary.

Following are the calculation results:

The maximum cylinder volume of the Ruska pump: *1179 ml*. (D_{piston} *= 50.48 mm*, l_{max} *= 250.00 mm*)

The minimum cylinder volume: *0 ml*. (Pump is empty)

Volume of the core plug: *44.2 ml* (assume the dimension of the core is: d_{core} *= 25.0 mm*, l_{core} *= 90.00 mm*, as used in this work).

The total volume of pipe, adapter, fittings and valves: *20 ml* (approximately).

Therefore the maximum volume in the system is *1179+44.2+20 = 1243.2 ml*. The volume of the rock could be ignored in the calculation if the rock permeability is reasonably low or the excitation frequency is very high.

The minimum volume is *44.2+20 = 64.2ml*, or *20ml* (ignore the rock size).

Water compressibility is $3.5 \sim 5 \times 10^{-5}$ */atm* or $2.4 \sim 3.4 \times 10^{-6}$ */psi*.

So according to:

$$C_w = \frac{1}{v} \times \left(\frac{\Delta v}{\Delta p} \right) \quad \textbf{(B-1)}$$

If the maximum injection pressure is *200 psi* and the excitation magnitude is *20%* of this value, then:

$$\Delta p = 40\, psi \quad \textbf{(B-2)}$$

Therefore:

$$c_w = \frac{1}{1243.2} \cdot \left(\frac{\Delta \mathrm{v}}{40} \right) = 3 \times 10^{-6} / psi \quad \textbf{(B-3)}$$

Hence:

$$\Delta v = 0.102 ml \quad \textbf{(B-4)}$$

The displacement of the exciter is *0.1 ~ 99.9 mm* (the displacement varies for different kind of exciters). Assume $\Delta l = 8mm$.

$$\Delta v = \pi \cdot \frac{d_{piston}^{\,2}}{4} \cdot \Delta l \quad \textbf{(B-5)}$$

Therefore,

$$d_{piston} = 4mm \quad \textbf{(B-6)}$$

The force needed to generate this displacement:

$$f_{mass} = p \cdot s \quad \textbf{(B-7)}$$

So:

$$f_{mass} = 240\, psi \cdot \frac{\pi}{4} \cdot \left(0.4 cm^2 \right) = \left(\frac{240}{14.5} \right) kg / cm^2 \cdot \frac{\pi}{4} \cdot \left(0.4 cm \right)^2 \quad \textbf{(B-8)}$$

Finally:

$$f_{mass} = 2.2kg \quad \textbf{(B-9)}$$

$$f_{force} = 20N \quad \textbf{(B-10)}$$

The calculation is based on the system volume at maximum state. One point that should be mentioned is that the system volume is changing during the test (the pump volume is decreasing during the injection, and the pump volume is the dominating factor in calculating the total volume).

To generate pressure pulses with different magnitude, the process of calculation is the same. The checking procedure is based on the maximum work power of the exciter. Therefore, once the exciter model is determined, to protect the exciter from losing efficiency, the maximum injecting pressure can not be greater than that in the derivation.

Appendix C

Labview Data Acquisition System

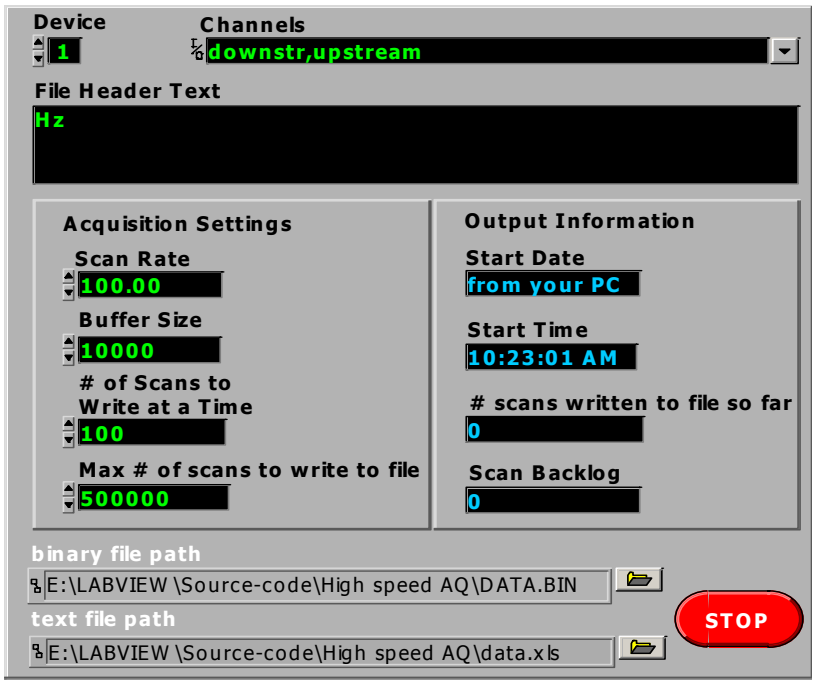

Figure C.1: Labview data acquisition system interface.

A Labview program has developed for data acquisition in this study. The user interface is friendly and self-explanatory as shown in Figure C.1. Currently, the upstream, downstream and differential pressure signals are recorded. The system can be expanded to 16-channel analog input. The theoretical maximum sampling speed is 200 kS/sec. To have a clear pressure trend record yet small data file size, moderate sampling speed (below 1000 samples/sec) is recommended. The file format output could be text document or to an Excel spreadsheet.